NATIONAL ADVISORY COMMITTEE FOR AERONAUTICS

TECHNICAL NOTE 3743

AN OPTIMUM SWITCHING CRITERION FOR A THIRD-ORDER CONTACTOR ACCELERATION CONTROL SYSTEM

By Anthony L. Passera and Ross G. Willoh, Jr.

Langley Aeronautical Laboratory
Langley Field, Va.

Washington

August 1956

NATIONAL ADVISORY COMMITTEE FOR AERONAUTICS

TECHNICAL NOTE 3743

AN OPTIMUM SWITCHING CRITERION FOR A THIRD-ORDER CONTACTOR ACCELERATION CONTROL SYSTEM

By Anthony L. Passera and Ross G. Willoh, Jr.

SUMMARY

A criterion for the optimum performance of a third-order contactor acceleration control system having complex roots is presented. This criterion determines the switching sequence of a contactor utilized to secure optimum performance and is hence called a switching criterion. Analytical and analog-computer methods are utilized to determine this criterion. The resulting optimum transient responses are presented and compared with those of a linear system. In order to introduce the methods involved, the switching criterion is first determined for a second-order system.

INTRODUCTION

Many recent advances in contactor servo theory have been directed toward the improvement of control-system transient responses. These improvements have resulted in systems with transient responses to step inputs of the controlled variable that reach steady-state values in a minimum of time with no transient overshoot. Such transient responses are called optimum responses.

An early paper by Flügge-Lotz and Klotter (ref. 1) applied anticipatory switching to contactor servomechanisms. In 1946, Weiss (ref. 2) presented a detailed phase-plane analysis of a second-order contactor servomechanism. McDonald (ref. 3) later determined a unique switching criterion for this second-order system. Kang and Fett (ref. 4) applied the concept of principal-coordinate phase space to nonlinear servo systems. This concept simplified the analysis of higher order systems. In 1953, Bushaw (ref. 5) presented an analysis of the switching curve in the phase plane which yields transient responses that reach steady state in a minimum of time. Bogner and Kazda (ref. 6) and Bogner (ref. 7) present a generalized method for obtaining an optimum switching criterion in higher order systems and apply these methods to a third-order system with real roots. This criterion requires that an element with contactor characteristics be actuated by a nonlinear function of the control-system error and its time derivatives in such a manner that the derivatives of the system output go to zero at the instant that the output variable arrives at a steady-state value.

The purpose of this study is to apply the method presented in reference 7 for determining the optimum switching criterion to a third-order system having complex conjugate roots. Furthermore, this paper presents a relatively simple analog-computer method for obtaining this criterion and the resulting optimum transient responses.

In order to introduce the methods involved, the switching criterion is first determined for a second-order system that is descriptive of an ideal missile roll control system. The methods are then applied to a third-order system that is descriptive of an ideal missile acceleration control system. The application of this method to this system is complicated by the presence of complex conjugate roots.

Transient responses of a third-order limited-linear system are also included in this paper. These transient responses present a basis of comparison for the optimum third-order contactor control systems.

SYMBOLS

B_0,B_1,B_2,B_3,B_4	constants of integration
b	constant coefficient in airframe normal-acceleration transfer function, radians/sec
C	nondimensionalized constant, c/b^2
c	constant coefficient in airframe normal-acceleration transfer function, $(\text{radians/sec})^2$
E	nondimensionalized system error
E_i	nondimensionalized system error input
g	acceleration due to gravity
$j = \sqrt{-1}$	
K_1	velocity constant of servomotor in normal-acceleration control system, deg/sec/volt
K_2	proportionality constant in limited-linear normal-acceleration control system, volts/g unit

K_3	feedback gain constant in limited-linear normal-acceleration control system, volts/g unit/sec^2
K_4	velocity constant of airframe transfer function in roll control system, deg/sec/deg
K_5	static gain constant of airframe transfer function in normal-acceleration control system, g units/deg
n	control-system normal-acceleration output signal, g units
n_i	control-system normal-acceleration input signal, g units
s	Laplace transform variable
T	roll-control-system or airframe time constant, sec
t	time, sec
w_n	coordinate of w phase space
w_{na}	locus of switching points in w_n space
Δ_a	forcing function for mathematical analysis
Δ_r	actuating signal for servomotor, volts
$\Delta = -\Delta_r$	
δ	control-surface deflection, deg
ϵ	control-system actuating signal, g units or deg
$\lambda_1, \lambda_2, \lambda_3$	characteristic roots of normal-acceleration control system
τ	dimensionless time
ϕ	control-system roll-angle output signal, deg
ϕ_i	control-system roll-angle input signal, deg

A dot over a quantity denotes the derivative with respect to time t.

A primed quantity denotes the derivative with respect to dimensionless time τ.

The subscript a is employed as a switching index ($a = 0, 1, 2,$ and 3).

The subscript n is employed as a coordinate index ($n = 1, 2,$ and 3).

DEFINITIONS

Contactor: A nonlinear element which has an output constant in magnitude with the sign of the input and, furthermore, has zero output when the input is zero.

Optimum transient response: A transient response that reaches the steady-state value in a minimum of time with no overshoot.

Switching criterion: The system conditions at which contactor reversal must take place to yield optimum transient responses.

Locus of first switching points: The locus of system coordinates required to define the first contactor reversal points in an optimum contactor control system.

Locus of second switching points: The locus of system coordinates required to define the second contactor reversal points in an optimum third-order contactor control system.

Zero trajectories: The phase-space trajectories passing through the origin.

SYSTEM DESCRIPTION

Second-Order System

A block diagram of the first system considered in this investigation is given in figure 1(a). This system is descriptive of a missile contactor roll control system. A step input ϕ_i to the system causes an error ϵ to be applied to the contactor element. The sign of this error signal actuates the contactor which then applies a step aileron deflection δ to the control surface. A reversal of the sign of the error signal when the error reaches zero causes a corresponding reversal of the contactor output. In order to facilitate the analysis, δ is limited to $\pm 1^{\circ}$. The magnitude of the aileron deflection is included in the airframe velocity constant. The performance of this system is characterized by a large initial overshoot and a decaying oscillation.

The contactor system of figure 1(a) was then modified by the inclusion of a computer element controlling the contactor input to cause an optimum system respnse. Figure 1(b) is a block diagram of the modified system. In response to a step input ϕ_i, this element actuates the contactor which applies a step aileron deflection δ to the airframe. Unlike the system of figure 1(a), the sign of δ is reversed before the error reaches zero. In the optimum case, the sign reversal takes place at the appropriate time to cause the error and the first time derivative of the error to reach zero simultaneously. The return of the control-surface servo to a neutral position removes the control-surface deflection, and the system remains at rest. The neutral relay position required to keep the system at rest is not shown in the block diagrams; therefore, figures 1(b) and 2 apply to the systems only when they are not at this rest or steady-state position.

Third-Order System

A block diagram of the optimum third-order contactor control system considered for this study is given in figure 2. The performance of this system is similar to that of the optimum second-order system previously described with the exception that, because of the order of the system, the computer element must actuate the contactor in such a manner that the error and its first two time derivatives go to zero simultaneously. In order to accomplish this, a minimum of two switchings is required. In response to a step input of acceleration, the contactor element of the optimum third-order system applies a constant rate of pitch control-surface deflection to the airframe. In a manner similar to the second-order system, the contactor output is restricted to ± 1 by including the actual magnitude of this output in the constant K_1. The resulting rate of control-surface deflection $\dot{\delta}$ causes the error to decrease at an increasing rate. Then, the contactor output is reversed. The error continues to decrease but with a decreasing rate. Once more reversal of the contactor output causes the error, the error rate, and error acceleration to go to zero simultaneously. Figure 3 illustrates a typical response of this system to a step input of the controlled variable. This figure contains time histories of ϵ, $\dot{\epsilon}$, $\ddot{\epsilon}$, Δ_r, and n_i.

Figure 4 is a block diagram of a limited-linear third-order normal-acceleration control system. The forward loop gain K_2 and the feedback gain K_3 of this system were adjusted to minimize $\int_0^t |\epsilon(t)| dt$ for a 5g step input.

METHOD OF ANALYSIS

The analysis is concerned with the determination of the switching criterion necessary for the optimum performance of a contactor control system. The mathematical analysis is based primarily on that developed by Bogner in reference 7. The transfer-function coefficients used for the systems discussed are presented in table I.

Second-Order System

The equation for the simple contactor roll control system shown in figure 1(a) can be written as

$$T \frac{d^2\phi}{dt^2} + \frac{d\phi}{dt} = K_4\delta \tag{1}$$

Inasmuch as $\epsilon = \phi_i - \phi$, if only step inputs of position are considered, equation (1) can be written:

$$T \frac{d^2\epsilon}{dt^2} + \frac{d\epsilon}{dt} = -K_4\delta \tag{2}$$

Substituting $\ddot{\epsilon} = \dot{\epsilon} \frac{d\dot{\epsilon}}{d\epsilon}$ and performing the integration yields

$$\frac{1}{T} \epsilon + \dot{\epsilon} - K_4\delta \log_e\left(\dot{\epsilon} + K_4\delta\right) = B_0 \tag{3}$$

where B_0 is the constant of integration. Equation (3) yields the phase portrait for the system from which any of the possible system trajectories may be obtained. For the system of figure 1(a), the sign of δ reverses as ϵ changes sign. A typical phase-plane plot of the response of the system to a step input of position obtained from an analog computer is shown in figure 5, and a transient response for this system is presented in figure 6.

Evaluation of the constant of integration B_0 in equation (3) for the phase-plane trajectories through the origin gives

$$\frac{1}{T}\epsilon + \dot{\epsilon} - K_4\delta \log_e\left(\frac{\dot{\epsilon}}{K_4\delta} + 1\right) = 0 \tag{4}$$

Because of the dual value of δ (that is, $\delta = \pm 1^{\circ}$), equation (4) is actually two equations:

$$\frac{1}{T}\epsilon + \dot{\epsilon} - K_4 \log_e\left(1 + \frac{\dot{\epsilon}}{K_4}\right) = 0 \tag{5a}$$

$$\frac{1}{T}\epsilon + \dot{\epsilon} + K_4 \log_e\left(1 - \frac{\dot{\epsilon}}{K_4}\right) = 0 \tag{5b}$$

Inasmuch as there exists only one solution of the equation $\frac{d\dot{\epsilon}}{d\epsilon} = f(\dot{\epsilon},\epsilon)$ through each point in the phase plane, equations (5a) and (5b) represent the only paths along which the representative point of the system may enter or leave the origin. These are called the zero trajectories.

Figure 7 shows zero trajectories obtained from equations (5a) and (5b) on an analog computer and by direct numerical substitution. Portions of these zero trajectories will later be used for the optimum system of figure 1(b). If equation (2) is set up on an analog computer, a phase-plane plot of $\dot{\epsilon}$ against ϵ obtained as the representative point moves from the origin with $\delta = +1^{\circ}$ will give curve oa of figure 7. Similarly, a solution of the same equation with $\delta = -1^{\circ}$ yields curve ob. The substitution of $-t$ for t in equation (2) results in the following equation:

$$T\frac{d^2\epsilon}{dt^2} - \frac{d\epsilon}{dt} = -K_4\delta \tag{6}$$

A phase-plane plot of $\dot{\epsilon}$ against ϵ obtained for equation (6) in a similar manner from an analog computer with $\delta = +1^{\circ}$ and $\delta = -1^{\circ}$ yields the curves oc and od, respectively, of figure 7. (See ref. 8.)

The segments of the zero trajectory od and oc entering the origin can be utilized as the contactor switching curve. If the sign of δ is reversed at the instant a system trajectory first intersects a segment of the zero trajectory entering the origin (at a point such as (a) in fig. 5), the system trajectory will then follow the zero trajectory to the origin and execute a deadbeat response. This switching criterion will yield an optimum transient response.

The block diagram of the second-order system, modified by the addition of a computer element to reverse the sign of δ when the representative point first intersects the switching curve, is presented in figure 1(b). This computer element senses the region of figure 7 in which the representative point of the system trajectory lies, and produces the proper contactor output. Whenever the representative point crosses the segment of the zero trajectory leading to the origin, the contactor output reverses. Finally, at the instant this point enters the origin, the contactor output goes to zero. Figure 7 also illustrates typical phase-plane responses of this system to step inputs of position, and figure 8, a number of transient responses obtained on an analog computer.

Third-Order System

In the second-order contactor system, the switching criterion causes ϵ and $\dot{\epsilon}$ to go to zero simultaneously. For an optimum third-order system, it can be shown that ϵ, $\dot{\epsilon}$, and $\ddot{\epsilon}$ must go to zero simultaneously. It is shown in reference 7 that two switchings are required to do this. In a third-order system the second or final switching curve in phase space leads to the origin and, hence, is still called the zero trajectory. In general, the locus of first switching points in a third-order system consists of a surface containing the zero trajectory. If, however, the inputs to the system are restricted to steps of the controlled variable, the locus of first switching points becomes a line lying in this surface.

In the following analysis the equation for the third-order system is presented. With the inputs restricted to steps of the controlled variable, a pair of simultaneous equations for the locus of first switching points is obtained. The zero trajectory is also developed from the equation for the system. An analog-computer method for obtaining this switching criterion is introduced and used to check the analytically derived criterion. Transient responses are then obtained from the contactor system using this switching criterion.

Analytical method.- A block diagram of the third-order contactor acceleration control system studied is given in figure 2. The differential equation of the basic system in terms of the error variable can be written as follows:

$$\dddot{\varepsilon}(t) + b\ddot{\varepsilon}(t) + c\dot{\varepsilon}(t) = K_1K_5c\ \Delta_r \tag{7a}$$

In the appendix, where a complete derivation of the switching criterion is presented, equation (7a) is nondimensionalized and written as

$$E'''(\tau) + E''(\tau) + CE'(\tau) = \Delta \tag{7b}$$

Equation (7b) is in general form inasmuch as time and amplitude scales may be adjusted for any desired undamped natural frequency and system velocity constant. The results obtained can be applied to any similar system with the same damping ratio (0.14).

In the following analysis, after two transformations of variables, the switching criterion is determined in terms of w_1, w_2, and w_3. These transformations were used to facilitate the analysis. The variables w_1, w_2, and w_3 are defined by the following three equations:

$$\left.\begin{aligned}
w_1(\tau) &= E(\tau) + \frac{1}{\lambda_2\lambda_3}E'(\tau) + \frac{1}{\lambda_2\lambda_3}E''(\tau) \\
w_2(\tau) &= -\frac{1}{\lambda_2\lambda_3}E'(\tau) - \frac{1}{\lambda_2\lambda_3}E''(\tau) \\
w_3(\tau) &= -j\frac{\lambda_3^2 + \lambda_2^2}{\lambda_2\lambda_3(\lambda_3 - \lambda_2)}E'(\tau) - j\frac{1}{\lambda_2\lambda_3(\lambda_3 - \lambda_2)}E''(\tau)
\end{aligned}\right\} \tag{8}$$

where the characteristic roots of the system are represented by λ.

In determining the loci of switching points, the variables w_{na} are introduced. The locus of first switching points will be written in terms of w_{11}, w_{21}, and w_{31} and the zero trajectory, or locus of second switching points, in terms of w_{12}, w_{22}, and w_{32} with both loci lying in the w_1, w_2, and w_3 phase space. It is shown in the appendix that the locus of first switching points can be represented by the following two equations:

$$1 + \frac{\lambda_3^2(\lambda_3 - \lambda_2)}{2\,\Delta_1}\left(w_{21} - jw_{31}\right) = \left[1 - \frac{\lambda_2^2(\lambda_3 - \lambda_2)}{2\,\Delta_1}\left(w_{21} + jw_{31}\right)\right]^{\lambda_3/\lambda_2} \tag{9}$$

and

$$1 \pm \sqrt{1 - \frac{\lambda_2^2(\lambda_3 - \lambda_2)}{2\,\Delta_1}\exp\left(w_{11}\frac{\lambda_2^2\lambda_3}{\Delta_1}\right)\left[w_{21} + jw_{31} + \frac{2\,\Delta_1}{\lambda_2^2(\lambda_3 - \lambda_2)}\right]} =$$

$$\left\{1 \pm \sqrt{1 + \frac{\lambda_3^2(\lambda_3 - \lambda_2)}{2\,\Delta_1}\exp\left(w_{11}\frac{\lambda_2\lambda_3^2}{\Delta_1}\right)\left[w_{21} - jw_{31} - \frac{2\,\Delta_1}{\lambda_3^2(\lambda_3 - \lambda_2)}\right]}\right\}^{\lambda_2/\lambda_3} \tag{10}$$

Figure 9 contains a plot in the w_3w_2 plane of values of w_{21} and w_{31} which satisfy equation (9). Inasmuch as equations (9) and (10) are simultaneous equations, the values of w_{21} and w_{31} which satisfy equation (9) were substituted point by point into equation (10), and the resulting equation solved for w_{11}. The values of w_{11} thus obtained are shown plotted against w_{21} and w_{31} in figures 10 and 11. This numerical evaluation was done with a digital computer. Figure 12 is a sketch of the locus of first switching points in the upper half of the w phase space.

It is further shown in the appendix that the locus of second switching points or zero trajectory can be expressed by the following pair of simultaneous equations:

$$\left(\lambda_2^2 + \lambda_3^2\right) - j\,\frac{\lambda_2^2\lambda_3^2(\lambda_3 - \lambda_2)}{\Delta_1}\,w_{32} = \lambda_3^2\exp\left(\frac{\lambda_2^2\lambda_3}{\Delta_1}\,w_{12}\right) + \lambda_2^2\exp\left(\frac{\lambda_2\lambda_3^2}{\Delta_1}\,w_{12}\right) \tag{11}$$

$$\left(\lambda_3^2 - \lambda_2^2\right) - \frac{\lambda_2^2\lambda_3^2(\lambda_3 - \lambda_2)}{\Delta_1} w_{22} = \lambda_3^2 \exp\left(\frac{\lambda_2^2\lambda_3}{\Delta_1} w_{12}\right) - \lambda_2^2 \exp\left(\frac{\lambda_2\lambda_3^2}{\Delta_1} w_{12}\right) \tag{12}$$

The w_1w_3 projection of the locus of second switching points is plotted in figure 13. Because the inputs are restricted to steps of the controlled variable, only the initial portion of this trajectory on either side of the origin is used.

Analog-computer method.- The two loci of switching points can be obtained by an analog-computer method. The determination of the switching criterion by this method involves the use of the original equation for the system (eq. (7b)) on an analog computer. Inasmuch as this equation is used, the criterion can be obtained in terms of the original system variables. However, for the presentation given here, the transformations of equations (8) were incorporated with equation (7b) in the analog-computer setup. This permitted the use of the analog-computer method to check the analytical results.

Transformed system coordinates: The actual determination of the switching criterion by an analog-computer method is accomplished in three steps. First, the zero trajectory or locus of second switching points is obtained. Second, the w_3w_2 projection of the locus of the first switching points is determined. Finally, after the complete space trajectory of the locus of second switching points and the w_3w_2 projection of the locus of first switching points are determined, the remaining w_1 coordinates of the locus of first switching points are obtained. In detail, this procedure is as follows:

(1) A solution is obtained in negative time from the origin of the w phase space with $\pm\Delta$. The resulting space curve is the path along which all trajectories entering the origin must travel. As in the second-order system, this space curve is called the zero trajectory.

(2) For step inputs $(w_1,0,0)$ to the system in positive time, all initial trajectories have the same w_3w_2 projection. Any subsequent switching from such initial trajectories must also have this projection. Hence, the w_3w_2 projection of the locus of first switching points is determined by operating the system in positive time with $\pm\Delta$ from the origin or any point on the w_1 axis and recording the w_3w_2 projection of the resulting trajectory.

(3) The zero trajectory and the w_3w_2 projection of the locus of first switching points have been determined. The w_1 values of the locus of second switching points remain to be found. Figure 14 shows the w_3w_2 projection of these two loci. If the system leaves the origin (point o of fig. 14) in negative time along the zero trajectory and Δ is switched at some point b between the origin and point a of curve oa, the value of w_1 recorded at the intersection of the resulting trajectory and the w_3w_2 projection of the locus of first switching points (points c, d, e, and f of fig. 14) is the remaining coordinate of this space curve. If the sign of Δ is again reversed at this intersection, the trajectory will follow the locus of first switching points to the origin. By varying the point on the zero trajectory where the system is first switched in negative time, the space curve of the locus of first switching points can be defined.

Values of the zero trajectory obtained by the method discussed are plotted in figure 13 along with solutions of the analytical expression. Projections of the locus of first switching points obtained with this method are shown with digital-computer solutions of the analytical expressions in figures 9, 10, and 11. It was found, during the analog-computer determination of the locus of first switching points, that the w_1 values associated with this space curve must be determined with care. Because of the switchings involved, it is possible to introduce considerable error at this point.

The phase-space operation of the system in response to a step input of the controlled variable is shown in figures 15 and 16. The phase-space trajectory begins with the initial value of error at point a. It travels along curve ab of these two figures until it intersects the locus of first switching points at b. At this point, the sign of Δ_r is reversed. This reversal changes the direction of the trajectory, which now travels along curve bc until the zero trajectory is reached at point c. Here the sign of Δ_r is again reversed and the system travels along the zero trajectory to the origin at point d.

Original-system coordinates: The analog method can be summarized in terms of its use to determine the switching criterion in terms of an original system error variable. The equation for the system is set up on the computer and a solution for $\epsilon(\tau)$ is obtained in negative time. The trajectory $\epsilon(-\tau) = f\left[\dot{\epsilon}(-\tau),\ \ddot{\epsilon}(-\tau),\ \Delta\right]$ obtained in this manner is the system locus of second switching points or zero trajectory. The equation of the system is then set up in positive time and the projection of the trajectory in the $\dot{\epsilon}(t)\ddot{\epsilon}(t)$ plane is recorded. This projection coincides with that of the locus of the first switching points in this plane. The remaining coordinate $\epsilon(t)$ is obtained by plotting the system trajectory on the $\dot{\epsilon}(t)\ddot{\epsilon}(t)$ plane as the system leaves the origin in negative time and then reversing the sign of Δ until the trajectory intercepts the previously mentioned projection plotted in positive time. The value of $\epsilon(t)$ at this intercept is the remaining required coordinate of the locus of first switching points. The procedure is repeated until sufficient points on this locus are established.

DISCUSSION OF THIRD-ORDER TRANSIENT RESPONSES

Transient responses obtained from the optimum contactor normal-acceleration control system for several step-input amplitudes are shown in figure 17. These responses are evaluated by comparison with those of an equivalent limited-linear system. The linear system utilized for this purpose is shown in the block diagram of figure 2. The maximum rate of control-surface deflection of the linear system was limited to that of the relay system. In addition, the forward loop gain K_2 and the feedback gain K_3 of the linear system were adjusted to minimize $\int_0^t |\epsilon(t)| dt$ for a step input of 5g. A series of transient responses obtained from this system for several step-input amplitudes are shown in figure 18. A comparison of figures 17 and 18 shows that in the optimum system overshoot is eliminated. In addition, this comparison also shows that there is a considerable superiority in rise time of the optimum system for input amplitudes below those at which the linear-system gains are adjusted. For larger input amplitudes, this superiority is less because the limited-linear system operates at its velocity saturation limit for a large percentage of the transient time. For the optimum case, the control surface, in response to a positive unit step input n_i, initially travels at a positive constant rate and then at the appropriate time travels at a negative rate. At the second switching point, the control surface travels at the positive constant rate again until the output n arrives at the steady-state value. This control-surface response is typical of the optimum contactor control system and is proportional to the integral of $\Delta_r(t)$ of figure 3.

CONCLUDING REMARKS

This paper presents a switching criterion that yields an optimum transient response to step inputs of the controlled variable for a third-order contactor system with complex roots. This optimum response has no overshoot and arrives at a steady-state value in a minimum of time in response to a step input of the controlled variable.

Two methods of obtaining this switching criterion, a direct mathematical method and the analog-computer method, are presented. In the direct mathematical method, two transformations of variables were applied to the original nondimensionalized equation of the system to determine the equations of the two loci of switching points in the phase space. The equations of these loci are in general form inasmuch as the time scale of the transient outputs as well as the amplitude scale may be adjusted for any desired undamped natural frequency and system velocity constant for the given value of damping ratio. A digital computer was utilized to obtain the actual coordinates of the switching loci after the equations of these loci were established.

The analog-computer method, although lacking the accuracy of the mathematical method, offers a relatively simple means of obtaining the two loci of switching points. In addition, these loci can be determined in terms of the original system error variable with no transformations.

The transient responses of the optimum system were compared with those of the equivalent limited-linear system. The optimum contactor acceleration control system is superior with respect to the time required to reach steady-state values; however, for large step inputs of the controlled variable, this time advantage is less because the limited-linear system operates at the velocity saturation limit for a large percentage of the transient time.

Langley Aeronautical Laboratory,
National Advisory Committee for Aeronautics,
Langley Field, Va., May 10, 1956.

APPENDIX

DERIVATION OF THIRD-ORDER SWITCHING CRITERION

Symbols

A matrix $\begin{bmatrix} 0 & 1 & 0 \\ 0 & 0 & 1 \\ 0 & -C & -1 \end{bmatrix}$

$G]$ matrix $\begin{bmatrix} 0 \\ 0 \\ \Delta \end{bmatrix}$

P transformation matrix

P^{-1} inverse matrix P

u_n coordinates in space $\frac{d^n}{d\tau^n}$ $(n = 1, 2, \text{and } 3)$

$u]$ matrix $\begin{bmatrix} u_1 \\ u_2 \\ u_3 \end{bmatrix}$

v_n principal coordinates of system $(n = 1, 2, \text{and } 3)$

$v]$ matrix $\begin{bmatrix} v_1 \\ v_2 \\ v_3 \end{bmatrix}$

$\beta = -j\sqrt{1 - 4C}$

Third-Order Switching Criterion

The basic form of the equation for the third-order system of figure 2 is

$$\frac{n}{\Delta_r} = \frac{K_1K_5c}{S(S^2 + bS + c)} \tag{A1}$$

When $\epsilon = n_i - n$ and inputs are restricted to steps of n_i so that $\dot{n}_i = \ddot{n}_i = \dddot{n}_i = 0$, equation (A1) can be written as follows:

$$\dddot{\epsilon}(t) + b\ddot{\epsilon}(t) + c\dot{\epsilon}(t) = -K_1K_5c\ \Delta_r \tag{A2}$$

This equation can be simplified with the following substitutions:

$$\Delta = -\Delta_r$$

$$\tau = bt$$

$$E(\tau) = \frac{b^3}{K_1K_5c}\ \epsilon(t)$$

$$C = \frac{c}{b^2}$$

This simplification results in

$$E'''(\tau) + E''(\tau) + CE'(\tau) = \Delta \tag{A3}$$

Let

$$\left.\begin{aligned} u_1 &= E(\tau) \\ u_2 &= E'(\tau) \\ u_3 &= E''(\tau) \end{aligned}\right\} \tag{A4}$$

From equations (A3) and (A4) the following equations can be written:

$$\left.\begin{aligned} \frac{du_1}{d\tau} &= u_2 \\ \frac{du_2}{d\tau} &= u_3 \\ \frac{du_3}{d\tau} &= -Cu_2 - u_3 + \Delta \end{aligned}\right\} \tag{A5}$$

In matrix notation, equations (A5) become

$$\frac{d}{d\tau}\begin{bmatrix} u_1 \\ u_2 \\ u_3 \end{bmatrix} = \begin{bmatrix} 0 & 1 & 0 \\ 0 & 0 & 1 \\ 0 & -C & -1 \end{bmatrix} \begin{bmatrix} u_1 \\ u_2 \\ u_3 \end{bmatrix} + \begin{bmatrix} 0 \\ 0 \\ \Delta \end{bmatrix} \tag{A6}$$

or

$$\frac{d}{d\tau} u\rfloor = A\ u\rfloor + G\rfloor \tag{A7}$$

The roots of the characteristic equation are

$$\lambda_1 = 0$$

$$\lambda_2 = \frac{-1 + \sqrt{1 - 4C}}{2}$$

$$\lambda_3 = \frac{-1 - \sqrt{1 - 4C}}{2}$$

When $j\beta = \sqrt{1 - 4C}$, these roots can be written as follows:

$$\left.\begin{aligned} \lambda_1 &= 0 \\ \lambda_2 &= \frac{-1 + j\beta}{2} \\ \lambda_3 &= \frac{-1 - j\beta}{2} \end{aligned}\right\} \tag{A8}$$

Introducing a new coordinate space $v]$ with the transformation matrix P so that

$$u] = P\, v] \tag{A9}$$

permits writing the system equation (A7) in terms of the new coordinates as follows:

$$\frac{d}{d\tau} v] = P^{-1}AP\, v] + P^{-1}\, G] \tag{A10}$$

When the principal-coordinate transformation is applied, the matrix P is determined so that the resulting $P^{-1}AP$ matrix is of the diagonal form. This selection results in (see ref. 7)

$$P = \begin{bmatrix} 1 & 1 & 1 \\ 0 & \lambda_2 & \lambda_3 \\ 0 & \lambda_2{}^2 & \lambda_3{}^2 \end{bmatrix} \tag{A11}$$

From equation (A11), where $-\left(\lambda_2 + \lambda_3\right) = 1$,

$$P^{-1} = \begin{bmatrix} 1 & \dfrac{1}{\lambda_3\lambda_2} & \dfrac{1}{\lambda_3\lambda_2} \\ 0 & \dfrac{\lambda_3}{\lambda_2\left(\lambda_3 - \lambda_2\right)} & \dfrac{-1}{\lambda_2\left(\lambda_3 - \lambda_2\right)} \\ 0 & \dfrac{-\lambda_2}{\lambda_3\left(\lambda_3 - \lambda_2\right)} & \dfrac{1}{\lambda_3\left(\lambda_3 - \lambda_2\right)} \end{bmatrix} \tag{A12}$$

After substitution of the values of equations (A11) and (A12) for the transformation matrix and its inverse, the matrix $P^{-1}AP$ can be evaluated as

$$P^{-1}AP = \begin{bmatrix} 0 & 0 & 0 \\ 0 & \lambda_2 & 0 \\ 0 & 0 & \lambda_3 \end{bmatrix} \tag{A13}$$

The substitution of equations (A12) and (A13) into equation (A10) gives

$$\frac{d}{d\tau}\begin{bmatrix} v_1 \\ v_2 \\ v_3 \end{bmatrix} = \begin{bmatrix} 0 & 0 & 0 \\ 0 & \lambda_2 & 0 \\ 0 & 0 & \lambda_3 \end{bmatrix}\begin{bmatrix} v_1 \\ v_2 \\ v_3 \end{bmatrix} + \begin{bmatrix} 1 & \frac{1}{\lambda_3\lambda_2} & \frac{1}{\lambda_3\lambda_2} \\ 0 & \frac{\lambda_3}{\lambda_2(\lambda_3 - \lambda_2)} & \frac{-1}{\lambda_2(\lambda_3 - \lambda_2)} \\ 0 & \frac{-\lambda_2}{\lambda_3(\lambda_3 - \lambda_2)} & \frac{1}{\lambda_3(\lambda_3 - \lambda_2)} \end{bmatrix}\begin{bmatrix} 0 \\ 0 \\ \Delta \end{bmatrix}$$

which is equivalent to

$$\frac{dv_1}{d\tau} = \frac{\Delta}{\lambda_3\lambda_2} \tag{A14}$$

$$\frac{dv_2}{d\tau} = \lambda_2 v_2 - \frac{\Delta}{\lambda_2(\lambda_3 - \lambda_2)} \tag{A15}$$

$$\frac{dv_3}{dt} = \lambda_3 v_3 + \frac{\Delta}{\lambda_3(\lambda_3 - \lambda_2)} \tag{A16}$$

Eliminating $d\tau$ between equations (A14) and (A15) and between equations (A14) and (A16) and integrating results in the following equations:

$$v_1 = \frac{\Delta}{\lambda_2{}^2\lambda_3} \log_e\left[\lambda_2 v_2 - \frac{\Delta}{\lambda_2(\lambda_3 - \lambda_2)}\right] + B_1 \tag{A17}$$

$$v_1 = \frac{\Delta}{\lambda_2\lambda_3^2} \log_e\left[\lambda_3 v_3 + \frac{\Delta}{\lambda_3(\lambda_3 - \lambda_2)}\right] + B_2 \tag{A18}$$

Equations (A17) and (A18) can be solved to yield a zero trajectory in terms of v_1, v_2, and v_3 and a locus of first switching points in terms of these same variables. These variables are, however, complex. In order to reduce these equations to real variables, it is first noted that equation (A9) when solved for $\left.v\right]$ yields

$$\left.v\right] = P^{-1} \left.u\right] \tag{A19}$$

The substitution of equation (A12) into equation (A19) leads to the following set of equations:

$$\left.\begin{aligned}
v_1 &= u_1 + \frac{1}{\lambda_2\lambda_3} u_2 + \frac{1}{\lambda_2\lambda_3} u_3 \\
v_2 &= \frac{\lambda_3}{\lambda_2(\lambda_3 - \lambda_2)} u_2 - \frac{1}{\lambda_2(\lambda_3 - \lambda_2)} u_3 \\
v_3 &= -\frac{\lambda_2}{\lambda_3(\lambda_3 - \lambda_2)} u_2 + \frac{1}{\lambda_3(\lambda_3 - \lambda_2)} u_3
\end{aligned}\right\} \tag{A20}$$

The substitution of equations (A8) into equations (A20) gives

$$\left.\begin{aligned}
v_1 &= u_1 + \frac{4}{\beta^2 + 1} u_2 + \frac{4}{\beta^2 + 1} u_3 \\
v_2 &= -\frac{2}{\beta^2 + 1} u_2 + j\frac{(1 - \beta^2)}{\beta(\beta^2 + 1)} u_2 - \frac{2}{\beta^2 + 1} u_3 + j\frac{2}{\beta(\beta^2 + 1)} u_3 \\
v_3 &= -\frac{2}{\beta^2 + 1} u_2 - j\frac{(1 - \beta^2)}{\beta(\beta^2 + 1)} u_2 - \frac{2}{\beta^2 + 1} u_3 - j\frac{2}{\beta(\beta^2 + 1)} u_3
\end{aligned}\right\} \tag{A21}$$

Inasmuch as v_2 and v_3 are complex conjugates and v_1 is a real variable, the following change of variables will yield equations in terms of real variables:

$$\left.\begin{aligned} w_1 &= v_1 \\ w_2 &= v_2 + v_3 \\ w_3 &= \frac{v_2 - v_3}{j} \end{aligned}\right\} \tag{A22}$$

Substituting equations (A22) into equations (A21) yields

$$\left.\begin{aligned} w_1 &= u_1 + \frac{4}{\beta^2 + 1} u_2 + \frac{4}{\beta^2 + 1} u_3 \\ w_2 &= -\frac{4}{\beta^2 + 1} u_2 - \frac{4}{\beta^2 + 1} u_3 \\ w_3 &= \frac{2(1 - \beta^2)}{\beta(\beta^2 + 1)} u_2 + \frac{4}{\beta(\beta^2 + 1)} u_3 \end{aligned}\right\} \tag{A23}$$

or, in terms of λ,

$$\left.\begin{aligned} w_1 &= u_1 + \frac{1}{\lambda_2\lambda_3} u_2 + \frac{1}{\lambda_2\lambda_3} u_3 \\ w_2 &= -\frac{1}{\lambda_2\lambda_3} u_2 - \frac{1}{\lambda_2\lambda_3} u_3 \\ w_3 &= -j \frac{{\lambda_3}^2 + {\lambda_2}^2}{\lambda_2\lambda_3(\lambda_3 - \lambda_2)} u_2 - j \frac{1}{\lambda_2\lambda_3(\lambda_3 - \lambda_2)} u_3 \end{aligned}\right\} \tag{A24}$$

Substituting equations (A22) into equations (A17) and (A18) yields

$$w_1 = \frac{\Delta}{\lambda_2{}^2\lambda_3} \log_e\left[\frac{\lambda_2}{2}\left(w_2 + jw_3\right) - \frac{\Delta}{\lambda_2\left(\lambda_3 - \lambda_2\right)}\right] + B_1 \tag{A25}$$

$$w_1 = \frac{\Delta}{\lambda_2\lambda_3{}^2} \log_e\left[\frac{\lambda_3}{2}\left(w_2 - jw_3\right) + \frac{\Delta}{\lambda_3\left(\lambda_3 - \lambda_2\right)}\right] + B_2 \tag{A26}$$

These two equations can be rewritten as follows:

$$\frac{w_2 + jw_3 - \dfrac{2\Delta}{\lambda_2{}^2\left(\lambda_3 - \lambda_2\right)}}{\exp\left(w_1 \dfrac{\lambda_2{}^2\lambda_3}{\Delta}\right)} = \frac{2}{\lambda_2} \exp\left(-B_1 \frac{\lambda_2{}^2\lambda_3}{\Delta}\right) = B_3 \tag{A27}$$

$$\frac{w_2 - jw_3 + \dfrac{2\Delta}{\lambda_3{}^2\left(\lambda_3 - \lambda_2\right)}}{\exp\left(w_1 \dfrac{\lambda_2\lambda_3{}^2}{\Delta}\right)} = \frac{2}{\lambda_3} \exp\left(-B_2 \frac{\lambda_2\lambda_3{}^2}{\Delta}\right) = B_4 \tag{A28}$$

A typical response of the system considered to a step input of the controlled variable will begin at $E(\tau) = E_i$, $E'(\tau) = 0$, and $E''(\tau) = 0$ and terminate at $E(\tau) = 0$, $E'(\tau) = 0$, and $E''(\tau) = 0$ in the $E(\tau)$ phase plane. The initial point of this response will be called 0, the first switching point 1, the second switching point 2, and the terminal point or origin 3. By using the transformations of equations (A24) and the notation that w_n at a point a along a trajectory becomes w_{na}, this response can be shown to begin at $w_1 = E_i = w_{10}$, $w_2 = 0$, $w_3 = 0$ and terminate at $w_1 = 0$, $w_2 = 0$, and $w_3 = 0$ in the w phase space. This response is shown schematically in the following diagram:

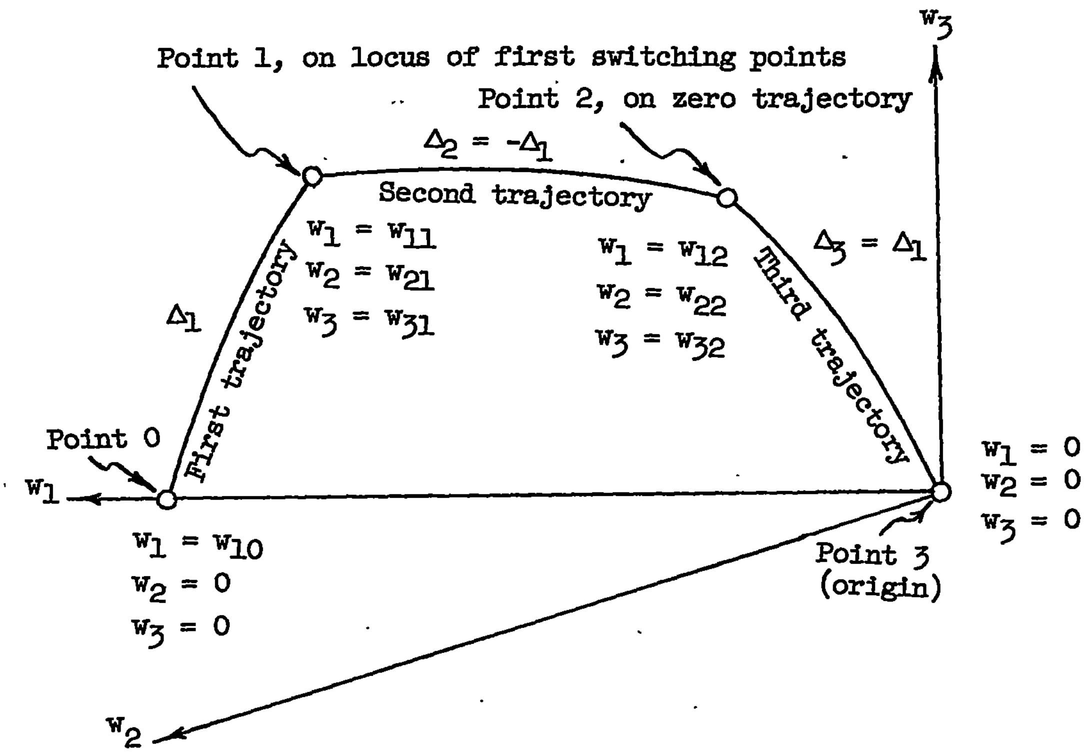

Pictorial diagram of typical w_n phase-space trajectory

The first trajectory of this diagram is described by equations (A27) and (A28) with Δ_1 substituted for Δ. The constants B_3 and B_4 have the same respective values at any point on this trajectory. If B_3 is evaluated from equation (A27) at point 0 and equated to B_3 evaluated at point 1 on this trajectory, the following equation can be written:

$$\frac{w_{21} + jw_{31} - \dfrac{2\Delta_1}{\lambda_2^2(\lambda_3 - \lambda_2)}}{\exp\left(w_{11}\dfrac{\lambda_2^2\lambda_3}{\Delta_1}\right)} = \frac{-\dfrac{2\Delta_1}{\lambda_2^2(\lambda_3 - \lambda_2)}}{\exp\left(w_{10}\dfrac{\lambda_2^2\lambda_3}{\Delta_1}\right)}$$

The application of this procedure to the three trajectories for both B_3 and B_4 results in the following six equations in terms of the initial and terminal points and the two switching points:

From initial trajectory,

$$\frac{w_{21} + jw_{31} - \dfrac{2\Delta_1}{\lambda_2^2(\lambda_3 - \lambda_2)}}{\exp\left(w_{11} \dfrac{\lambda_2^2\lambda_3}{\Delta_1}\right)} = \frac{-\dfrac{2\Delta_1}{\lambda_2^2(\lambda_3 - \lambda_2)}}{\exp\left(w_{10} \dfrac{\lambda_2^2\lambda_3}{\Delta_1}\right)} \tag{A29}$$

$$\frac{w_{21} - jw_{31} + \dfrac{2\Delta_1}{\lambda_3^2(\lambda_3 - \lambda_2)}}{\exp\left(w_{11} \dfrac{\lambda_2\lambda_3^2}{\Delta_1}\right)} = \frac{\dfrac{2\Delta_1}{\lambda_3^2(\lambda_3 - \lambda_2)}}{\exp\left(w_{10} \dfrac{\lambda_2\lambda_3^2}{\Delta_1}\right)} \tag{A30}$$

from second trajectory,

$$\frac{w_{21} + jw_{31} + \dfrac{2\Delta_1}{\lambda_2^2(\lambda_3 - \lambda_2)}}{\exp\left(-w_{11} \dfrac{\lambda_2^2\lambda_3}{\Delta_1}\right)} = \frac{w_{22} + jw_{32} + \dfrac{2\Delta_1}{\lambda_2^2(\lambda_3 - \lambda_2)}}{\exp\left(-w_{12} \dfrac{\lambda_2^2\lambda_3}{\Delta_1}\right)} \tag{A31}$$

$$\frac{w_{21} - jw_{31} - \dfrac{2\Delta_1}{\lambda_3^2(\lambda_3 - \lambda_2)}}{\exp\left(-w_{11} \dfrac{\lambda_2\lambda_3^2}{\Delta_1}\right)} = \frac{w_{22} - jw_{32} - \dfrac{2\Delta_1}{\lambda_3^2(\lambda_3 - \lambda_2)}}{\exp\left(-w_{12} \dfrac{\lambda_2\lambda_3^2}{\Delta_1}\right)} \tag{A32}$$

and from zero trajectory,

$$\frac{w_{22} + jw_{32} - \dfrac{2\Delta_1}{\lambda_2^2(\lambda_3 - \lambda_2)}}{\exp\left(w_{12} \dfrac{\lambda_2^2\lambda_3}{\Delta_1}\right)} = -\frac{2\Delta_1}{\lambda_2^2(\lambda_3 - \lambda_2)} \tag{A33}$$

$$\frac{w_{22} - jw_{32} + \dfrac{2\Delta_1}{\lambda_3^2(\lambda_3 - \lambda_2)}}{\exp\left(w_{12}\,\dfrac{\lambda_2\lambda_3^2}{\Delta_1}\right)} = \frac{2\Delta_1}{\lambda_3^2(\lambda_3 - \lambda_2)} \tag{A34}$$

The elimination of w_{12}, w_{22}, and w_{32} from equations (A29) to (A34) yields the following two simultaneous equations in terms of w_{11}, w_{21}, and w_{31}:

$$1 + \frac{\lambda_3^2(\lambda_3 - \lambda_2)}{2\Delta_1}\left(w_{21} - jw_{31}\right) = \left[1 - \frac{\lambda_2^2(\lambda_3 - \lambda_2)}{2\Delta_1}\left(w_{21} + jw_{31}\right)\right]^{\lambda_3/\lambda_2} \tag{A35}$$

and

$$1 \pm \sqrt{1 - \frac{\lambda_2^2(\lambda_3 - \lambda_2)}{2\Delta_1}\exp\left(w_{11}\,\frac{\lambda_2^2\lambda_3}{\Delta_1}\right)\left[w_{21} + jw_{31} + \frac{2\Delta_1}{\lambda_2^2(\lambda_3 - \lambda_2)}\right]} =$$

$$\left\{1 \pm \sqrt{1 + \frac{\lambda_3^2(\lambda_3 - \lambda_2)}{2\Delta_1}\exp\left(w_{11}\,\frac{\lambda_2\lambda_3^2}{\Delta_1}\right)\left[w_{21} - jw_{31} - \frac{2\Delta_1}{\lambda_3^2(\lambda_3 - \lambda_2)}\right]}\right\}^{\lambda_2/\lambda_3} \tag{A36}$$

Inasmuch as w_{11}, w_{21}, and w_{31} represent the first switching point, these two equations express the locus of first switching points.

Equations (A33) and (A34) can be manipulated to yield the w_1w_2 and the w_2w_3 projections of the zero trajectory as follows:

$$\left(\lambda_2^2 + \lambda_3^2\right) - j\,\frac{\lambda_2^2\lambda_3^2(\lambda_3 - \lambda_2)}{\Delta_1}\,w_{32} = \lambda_3^2\exp\left(\frac{\lambda_2^2\lambda_3}{\Delta_1}\,w_{12}\right) + \lambda_2^2\exp\left(\frac{\lambda_2\lambda_3^2}{\Delta_1}\,w_{12}\right) \tag{A37}$$

and

$$\left(\lambda_3^2 - \lambda_2^2\right) - \frac{\lambda_2^2\lambda_3^2\left(\lambda_3 - \lambda_2\right)}{\Delta_1} w_{22} = \lambda_3^2 \exp\left(\frac{\lambda_2^2\lambda_3}{\Delta_1} w_{12}\right) -$$

$$\lambda_2^2 \exp\left(\frac{\lambda_2\lambda_3^2}{\Delta_1} w_{12}\right) \qquad \text{(A38)}$$

REFERENCES

1. Flügge-Lotz, I., and Klotter, K.: On the Motions of an Oscillating System Under the Influence of Flip-Flop Controls. NACA TM 1237, 1949.

2. Weiss, Herbert K.: Analysis of Relay Servomechanisms. Jour. Aero. Sci., vol. 13, no. 7, July 1946, pp. 364-376.

3. McDonald, Donald: Nonlinear Techniques for Improving Servo Performance. Proc. Nat. Electronics Conf. (Chicago, Ill., 1950), vol. VI, 1951, pp. 400-421.

4. Kang, Chi Lung, and Fett, Gilbert H.: Metrization of Phase Space and Nonlinear Servo Systems. Jour. Appl. Phys., vol. 24, no. 1, Jan. 1953, pp. 38-41.

5. Bushaw, Donald Wayne: Differential Equations With a Discontinuous Forcing Term. Rep. No. 469, Exp. Towing Tank, Stevens Inst. Tech., 1953.

6. Bogner, Irving, and Kazda, Louis F.: An Investigation of the Switching Criteria for Higher Order Contactor Servomechanisms. Applications and Industry, no. 13, July 1954, pp. 118-127.

7. Bogner, I.: Basic Research in Nonlinear Mechanics As Applied to Servomechanisms. An Investigation of the Switching Criteria for Higher Order Contactor Servomechanisms. Interim Progress Rep. No. PR 16-9, Cook Electric Co. (Contract No. AF 33(038)-21673), Aug. 1953. (Available from ASTIA as AD No. 24023.)

8. Preston, John L.: Nonlinear Control of a Saturating Third-Order Servomechanism. Tech. Memo. No. 6897-TM-14 (Contract NOrd 11799), M.I.T., Servomechanisms Lab., 1954.

TABLE I.- TRANSFER-FUNCTION COEFFICIENTS

b, radians/sec	6.65
c, (radians/sec)^2	518
K_1, deg/sec/volt	14.0
K_2, volts/g unit	0.317
K_3, volts/g unit/sec^2	0.47
K_4, deg/sec/deg	1,000
K_5, g units/deg	903
T, sec	0.1

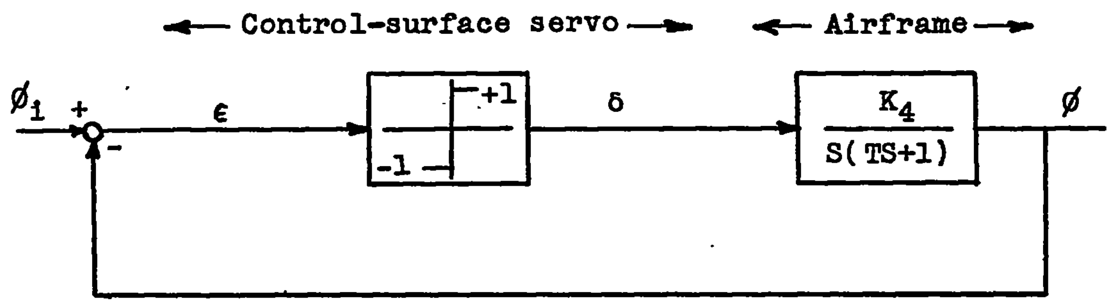

(a) Contactor roll control system.

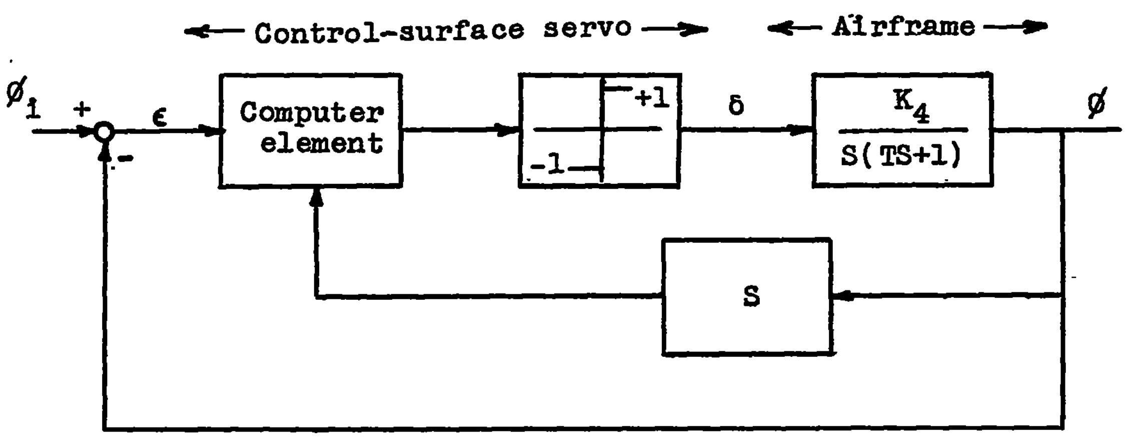

(b) Optimum contactor roll control system.

Figure 1.- Block diagrams of the contactor and the optimum contactor second-order roll control systems.

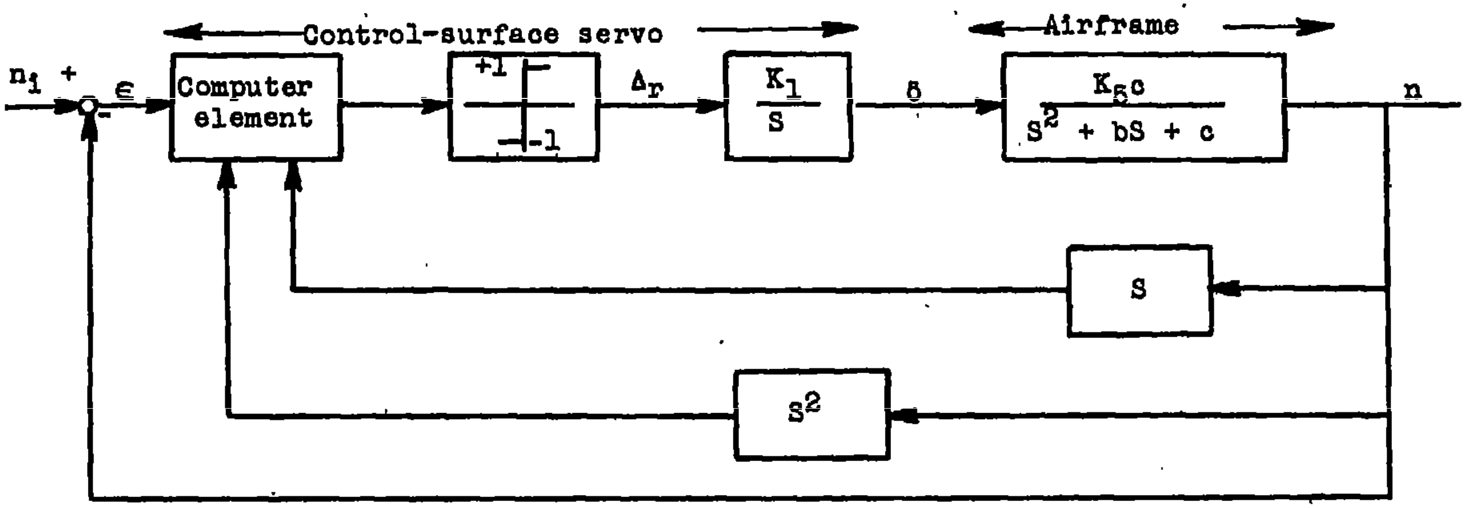

Figure 2.- Block diagram of the optimum third-order contactor normal-acceleration control system.

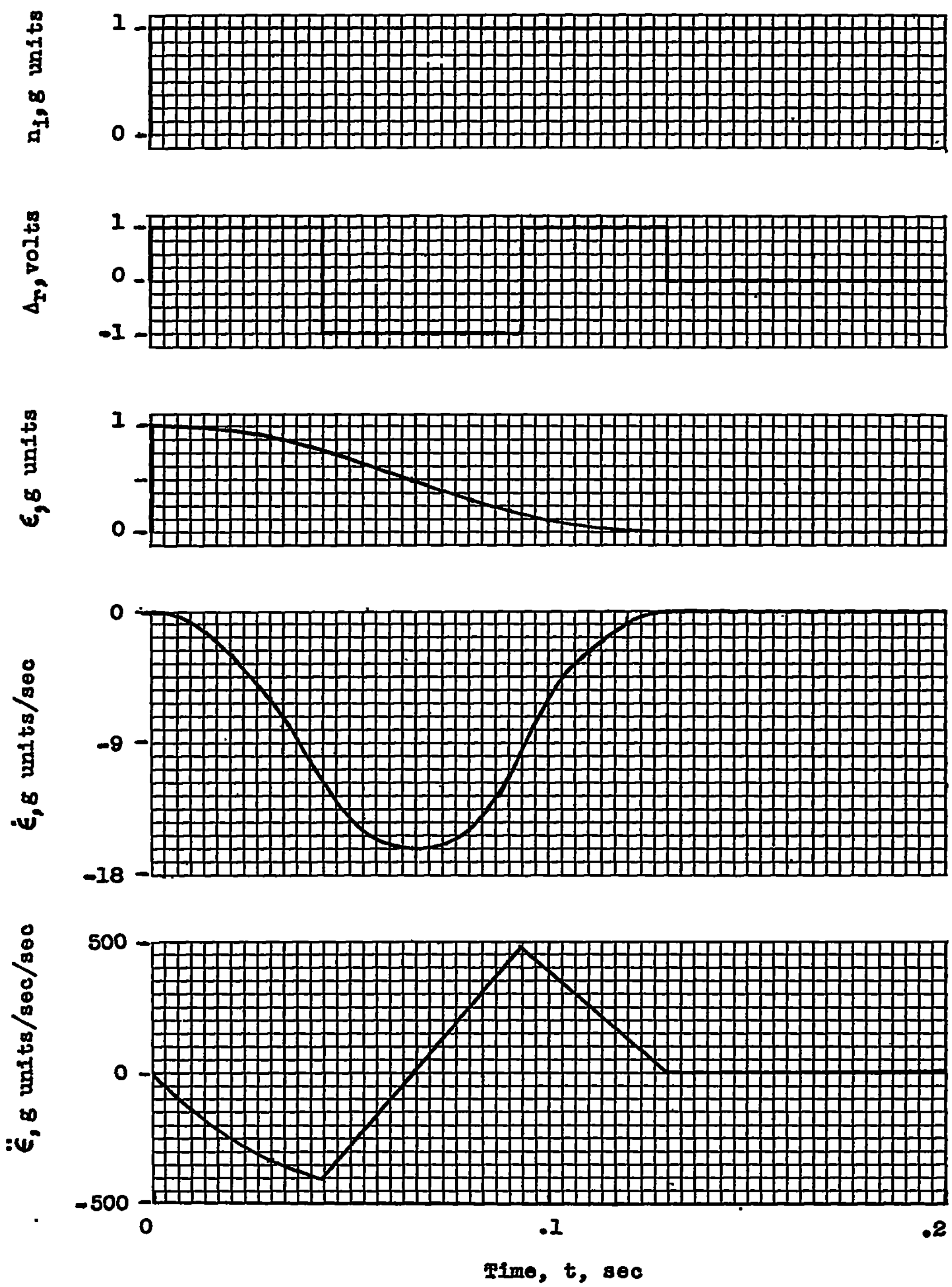

Figure 3.- Typical response of the third-order contactor acceleration control system to a step command signal.

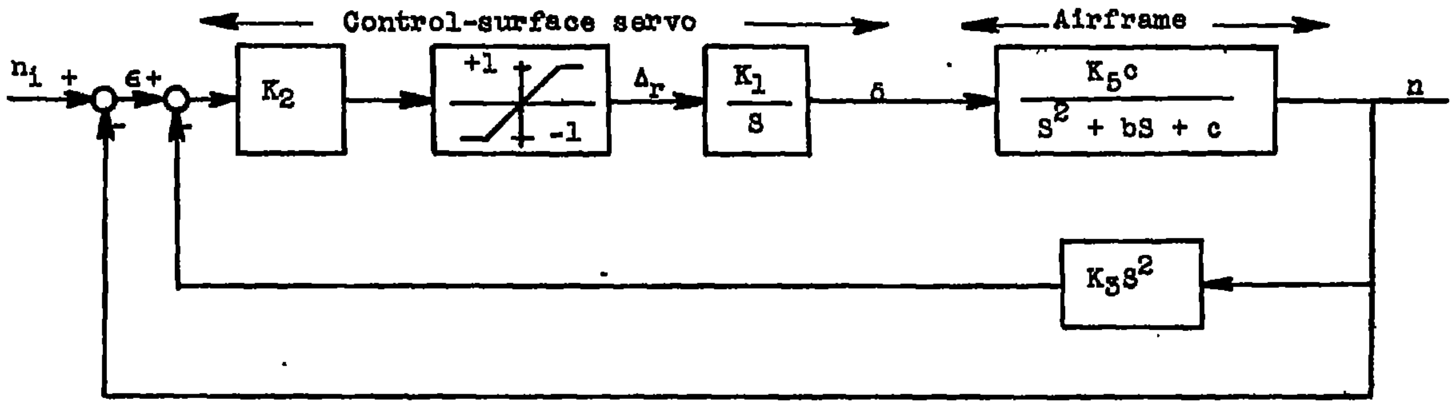

Figure 4.- Block diagram of the limited-linear normal-acceleration control system.

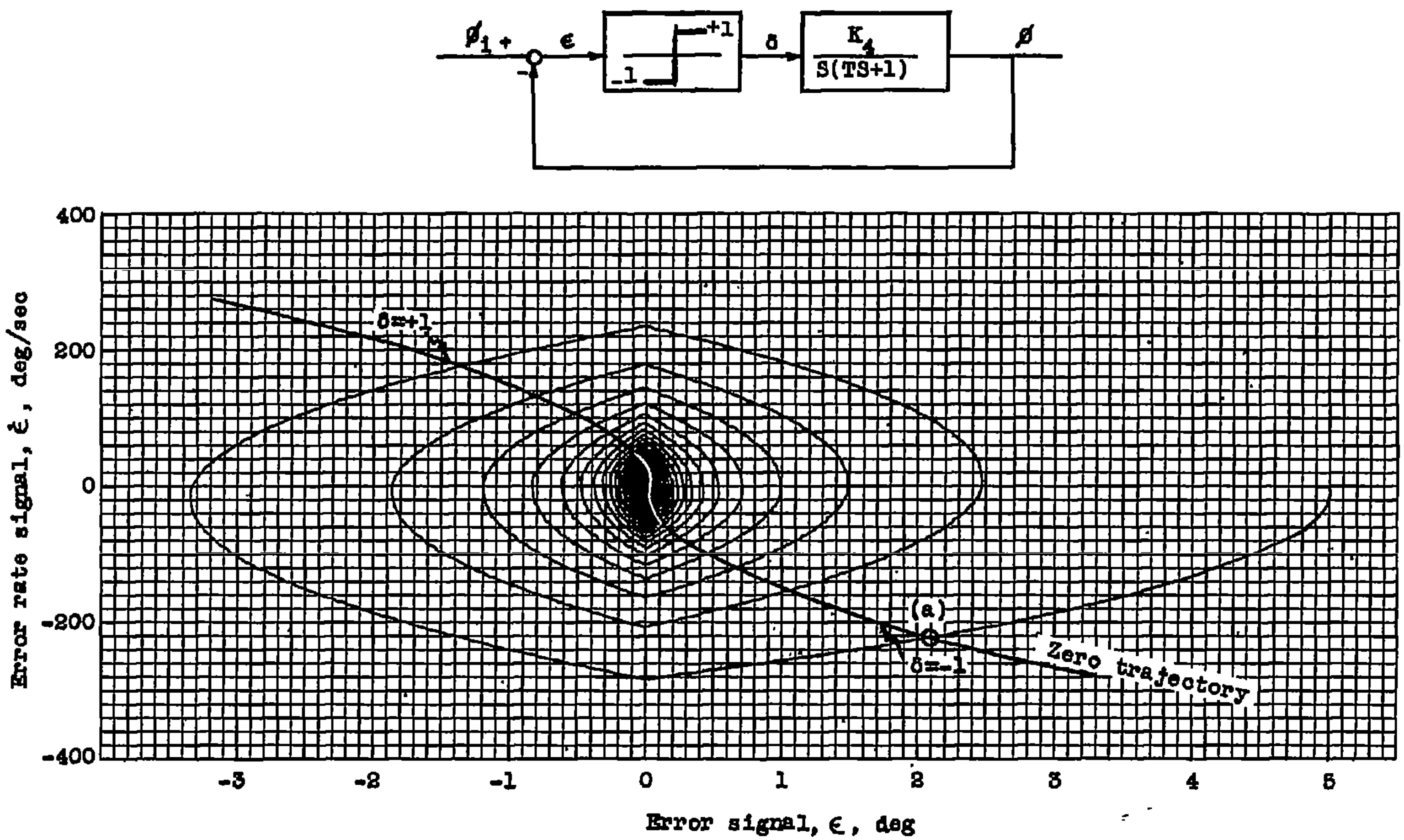

Figure 5.- A phase-plane plot of the contactor roll control system in response to a 5° step input. The zero trajectory for this system is superimposed on the plane.

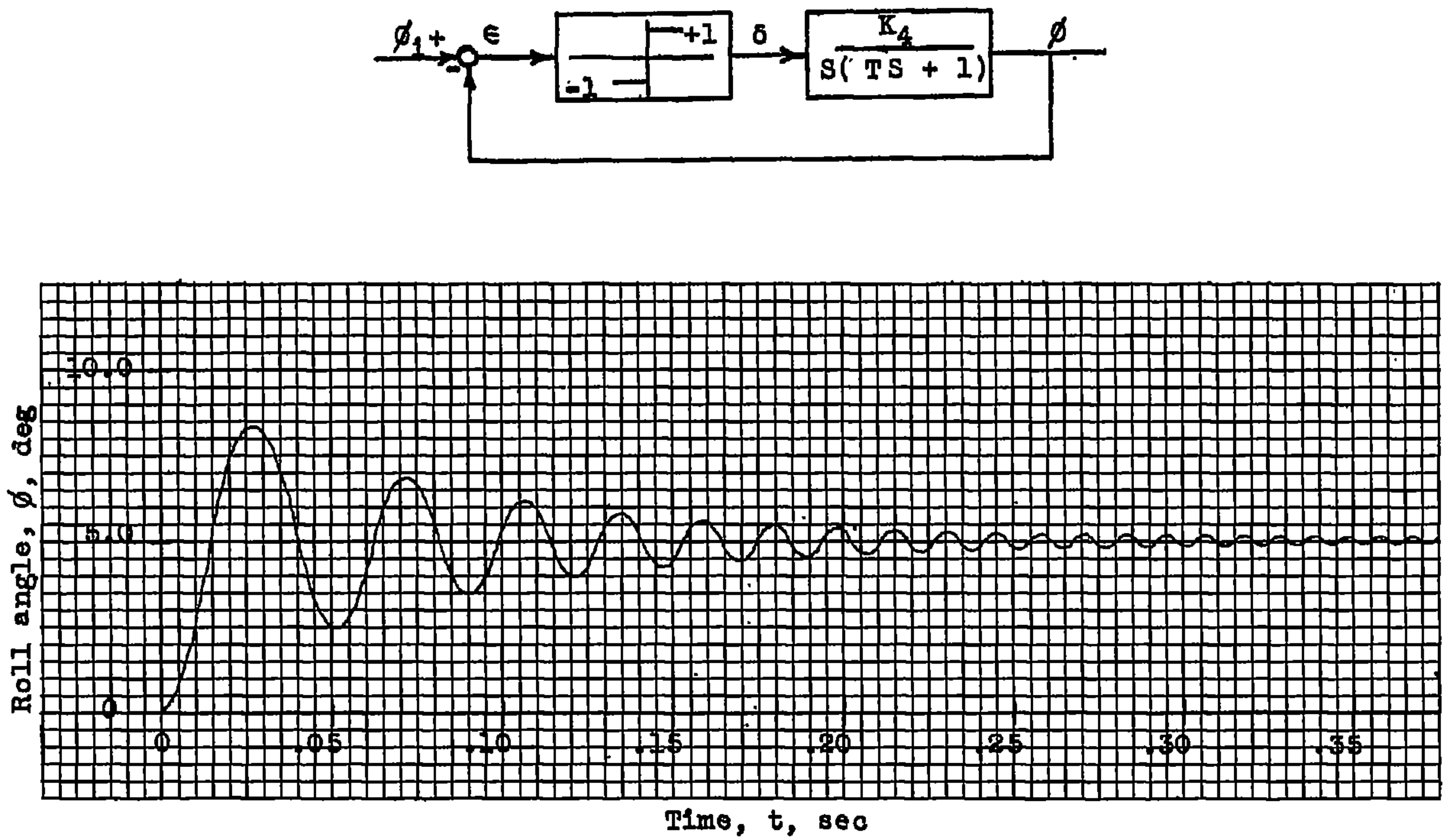

Figure 6.- Transient response of the contactor roll control system to a 5° step input.

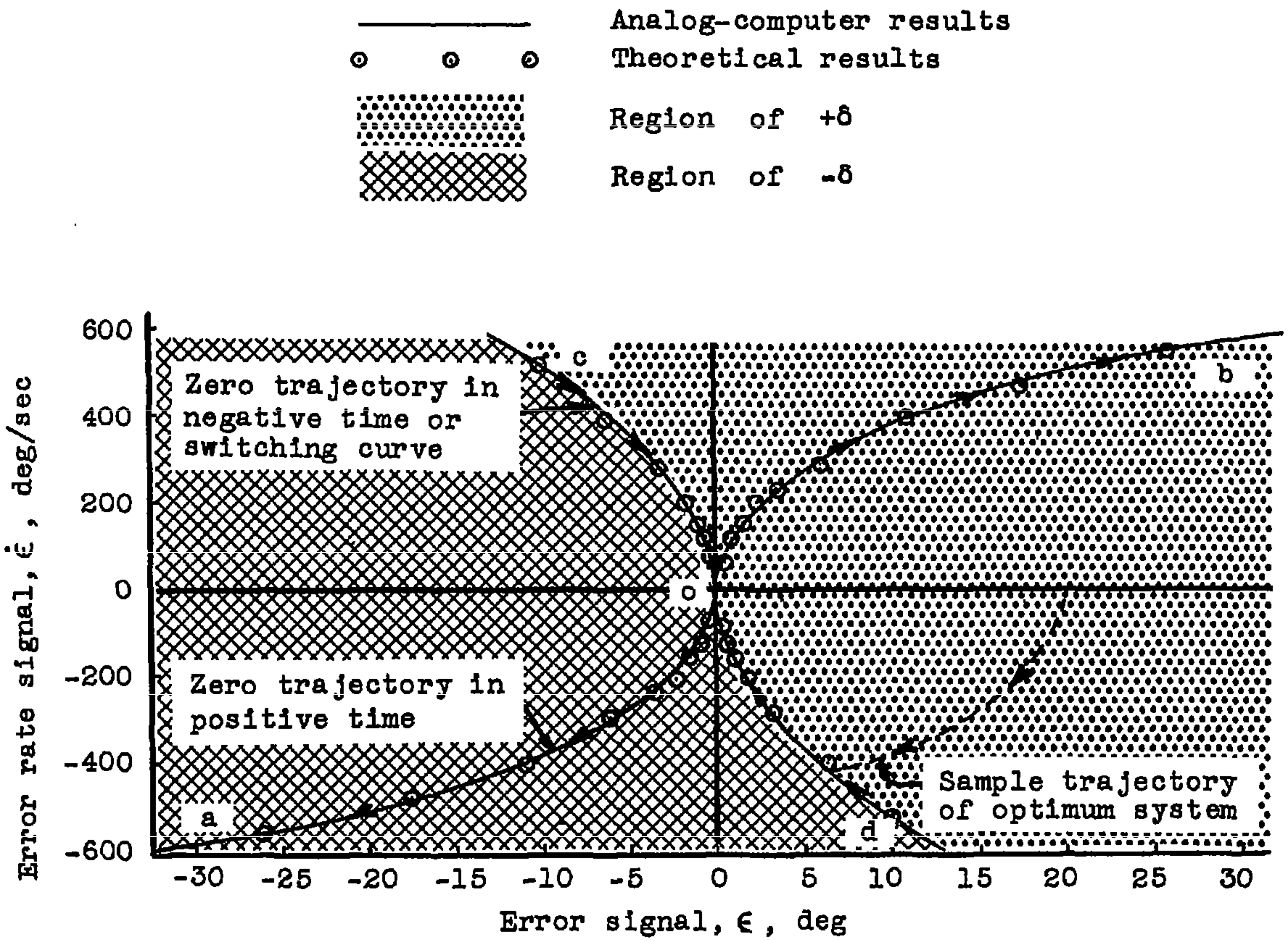

Figure 7.- Plot of the zero trajectories of the contactor roll control system on the phase plane.

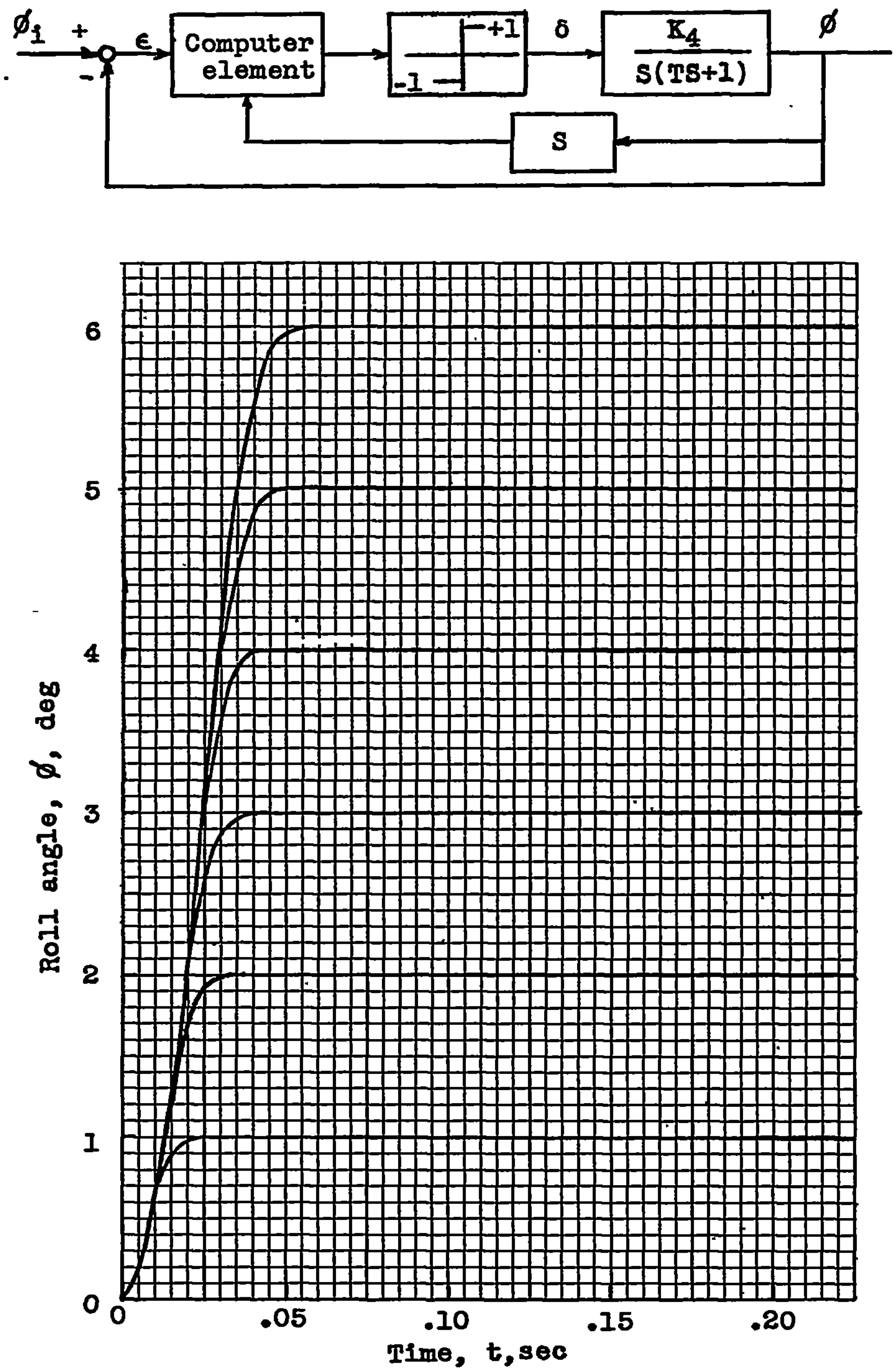

Figure 8.- Transient responses of the optimum contactor roll control system for step roll-angle inputs.

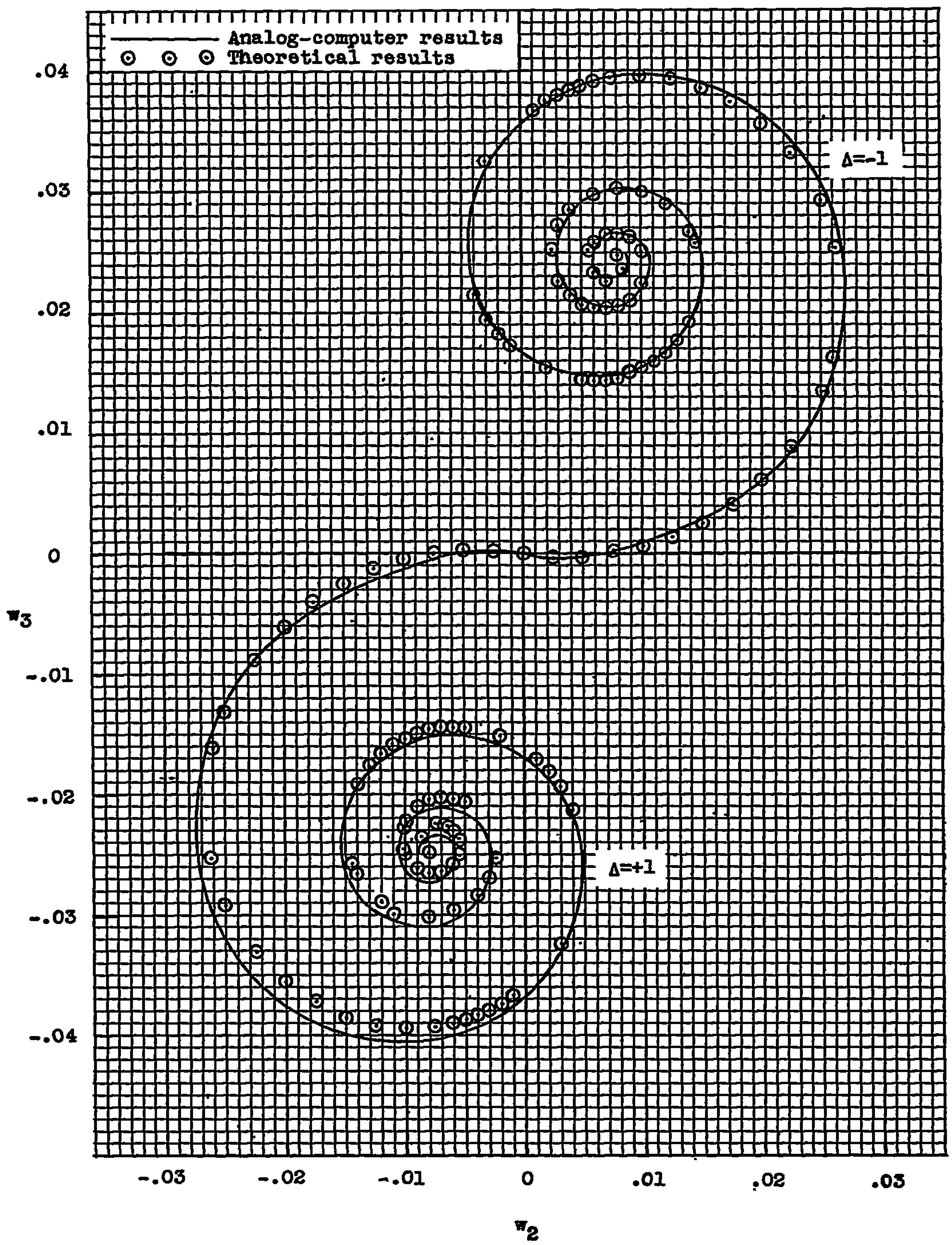

Figure 9.- Initial switching curve in the w_3w_2 plane of the optimum contactor normal-acceleration control system.

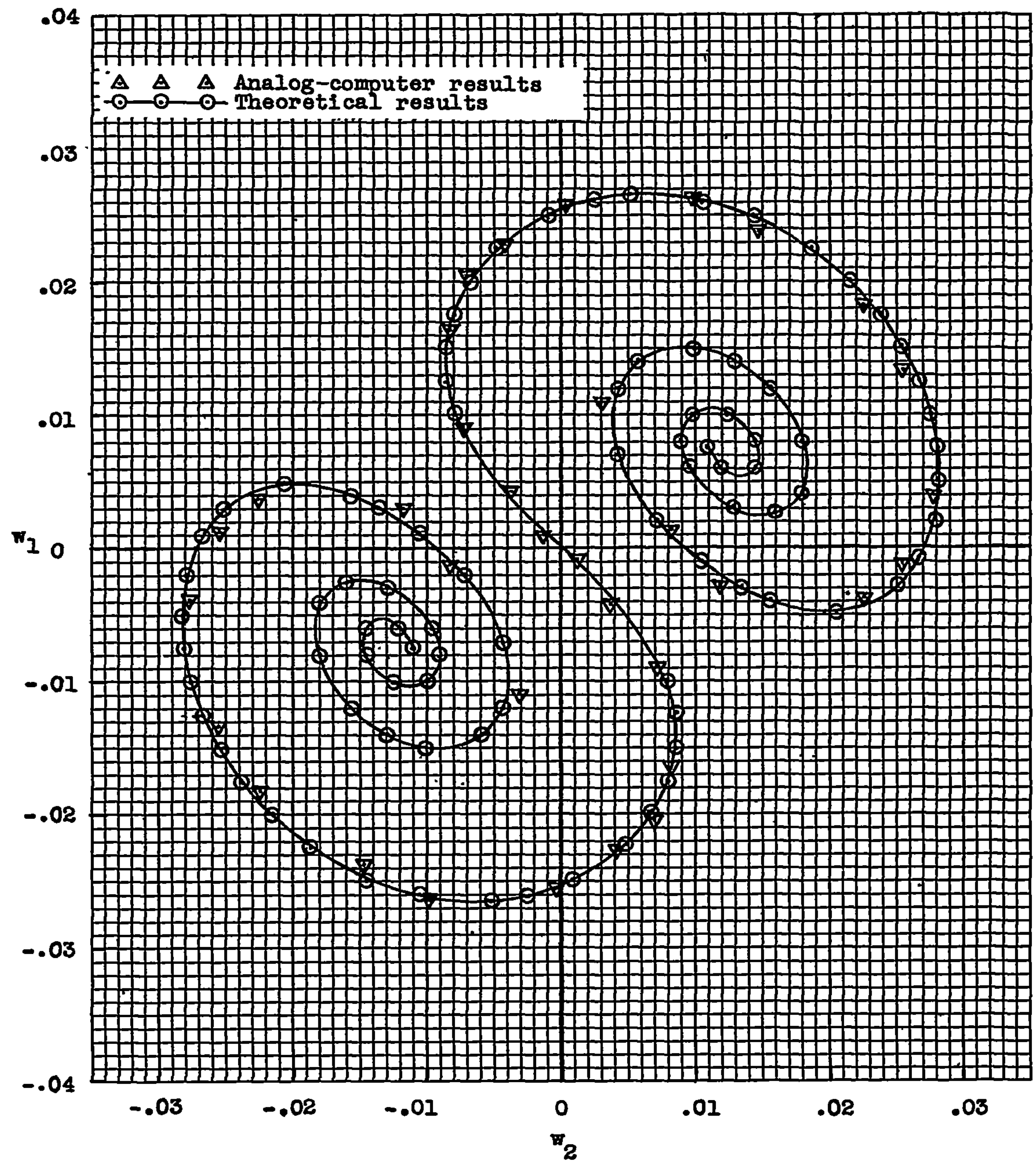

Figure 10.- Initial switching curve in the w_1w_2 plane for the optimum contactor normal-acceleration control system.

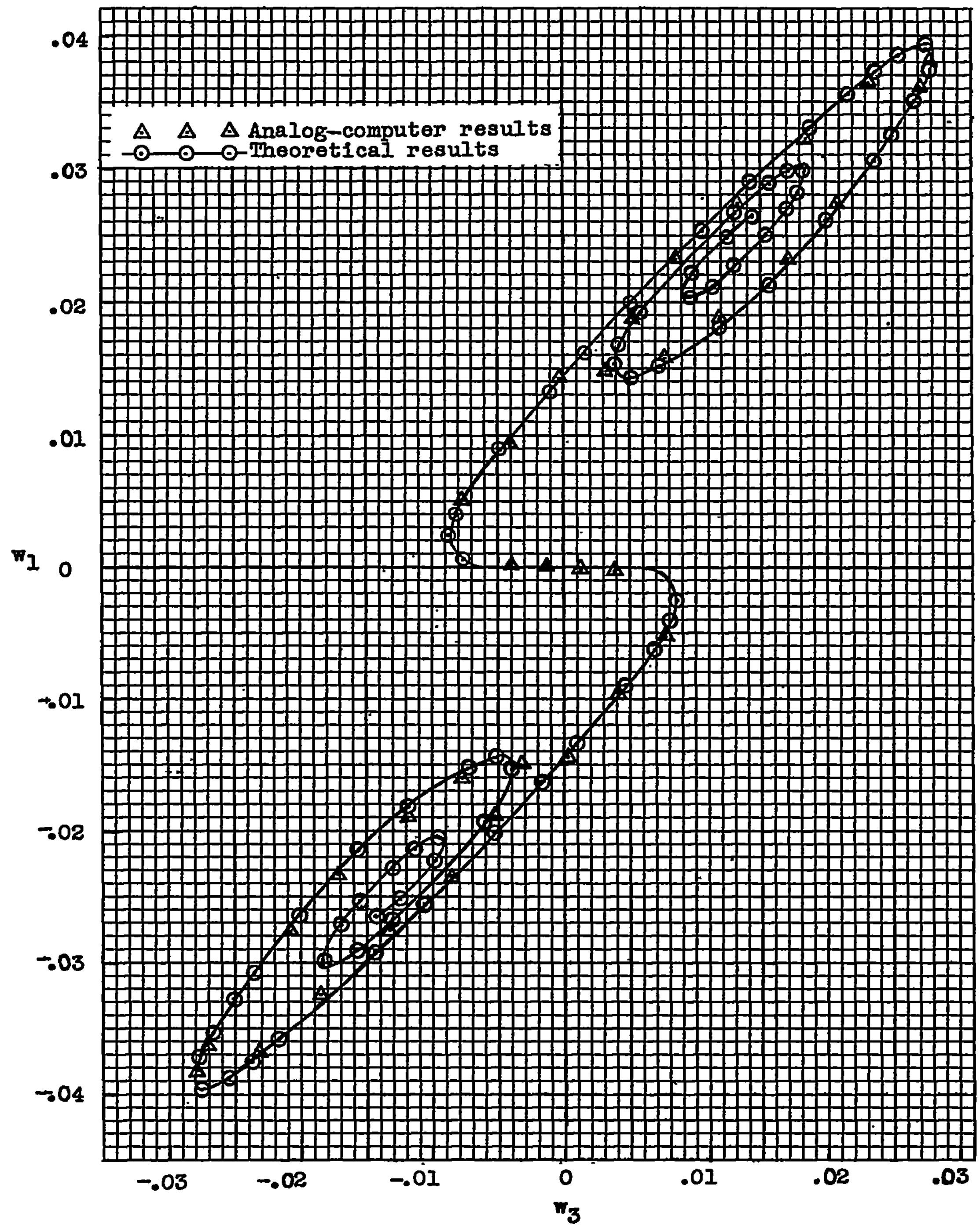

Figure 11.- Initial switching curve in the w_1w_3 plane for the optimum contactor normal-acceleration control system.

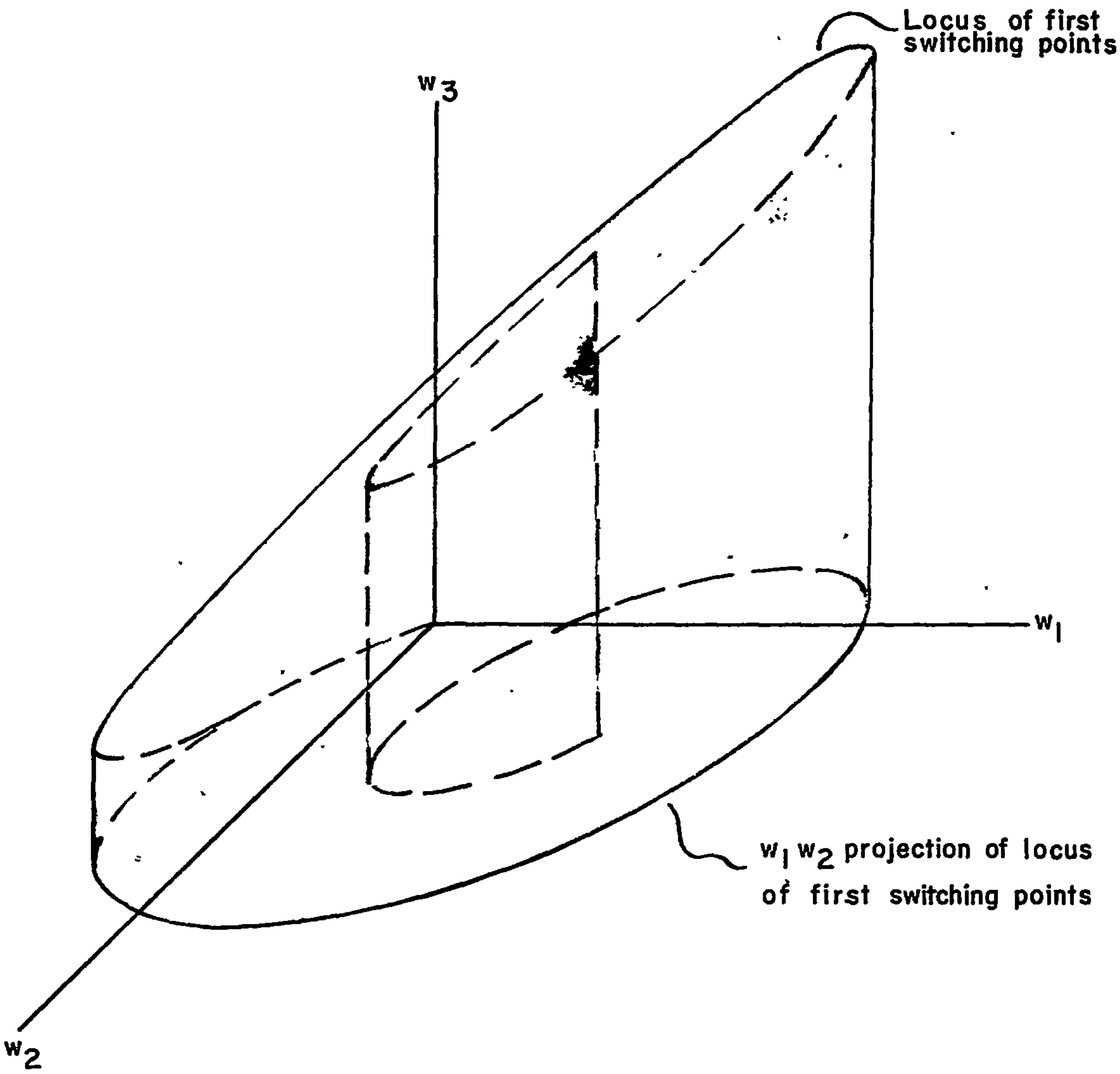

Figure 12.- Locus of first switching points in the upper half of the w phase space of the contactor normal-acceleration control system.

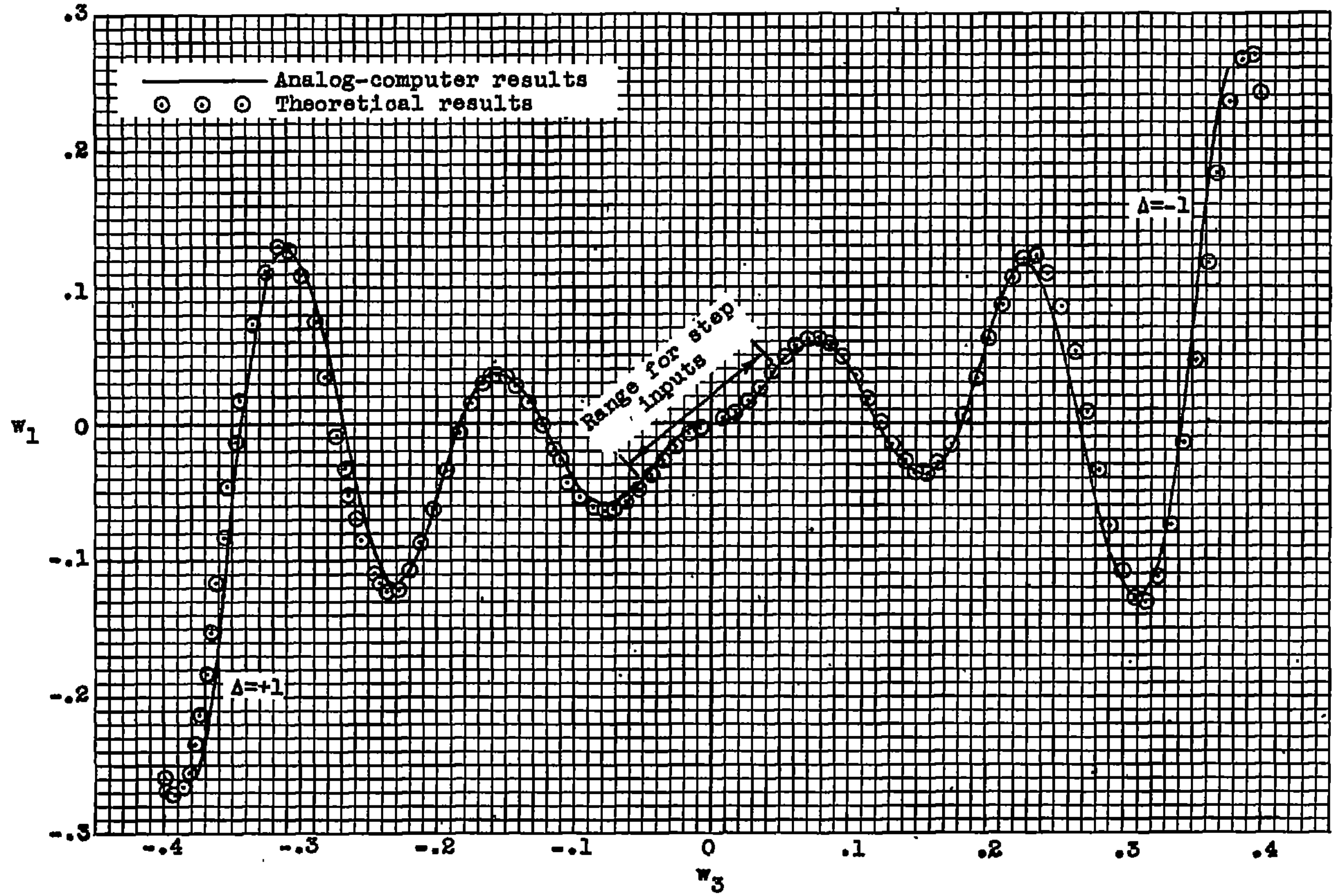

Figure 13.- Zero trajectory for the optimum contactor normal-acceleration control system.

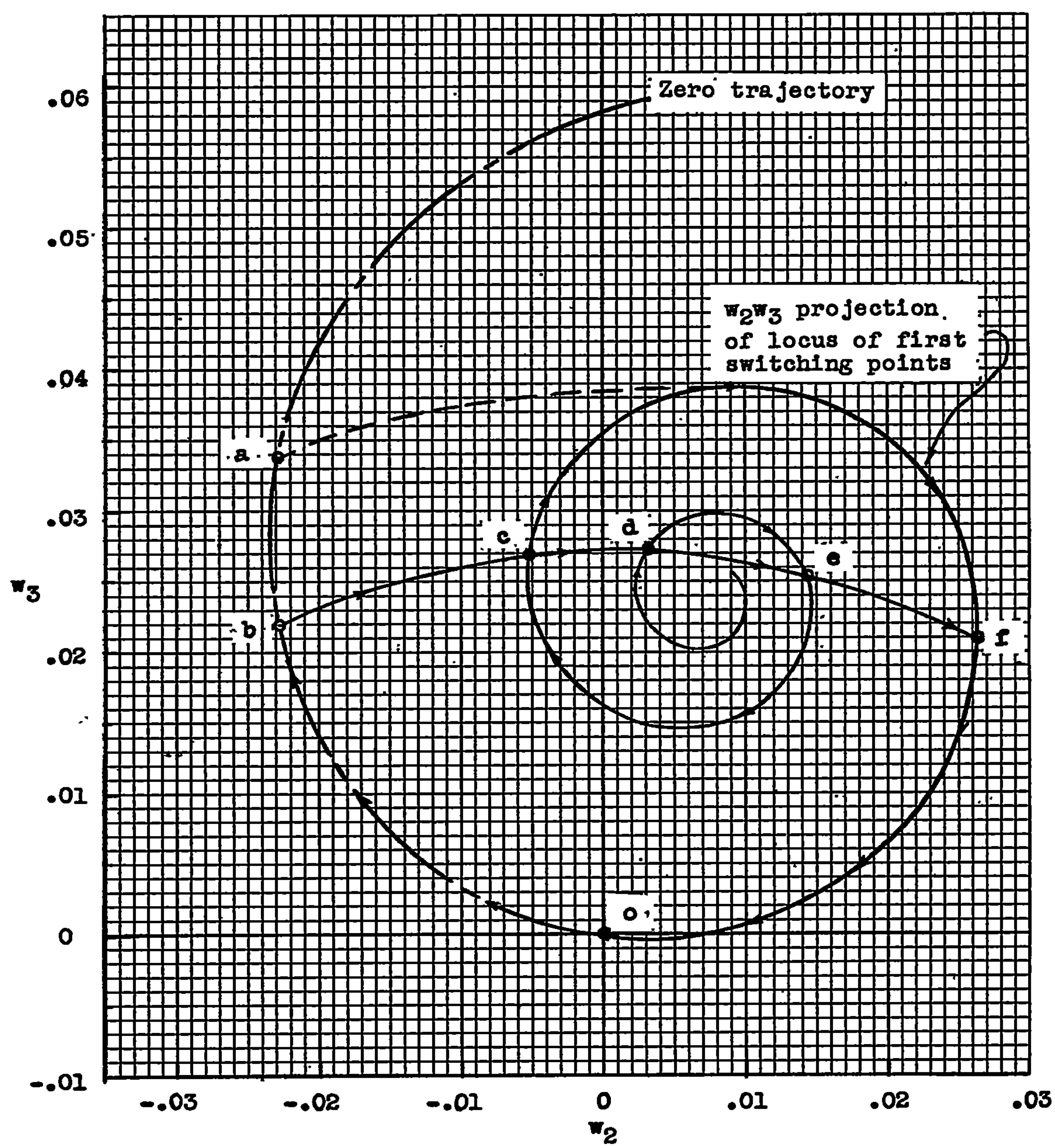

Figure 14.- A phase-plane plot illustrating the method of determining points on the first switching locus with an analog computer for the optimum contactor normal-acceleration control system.

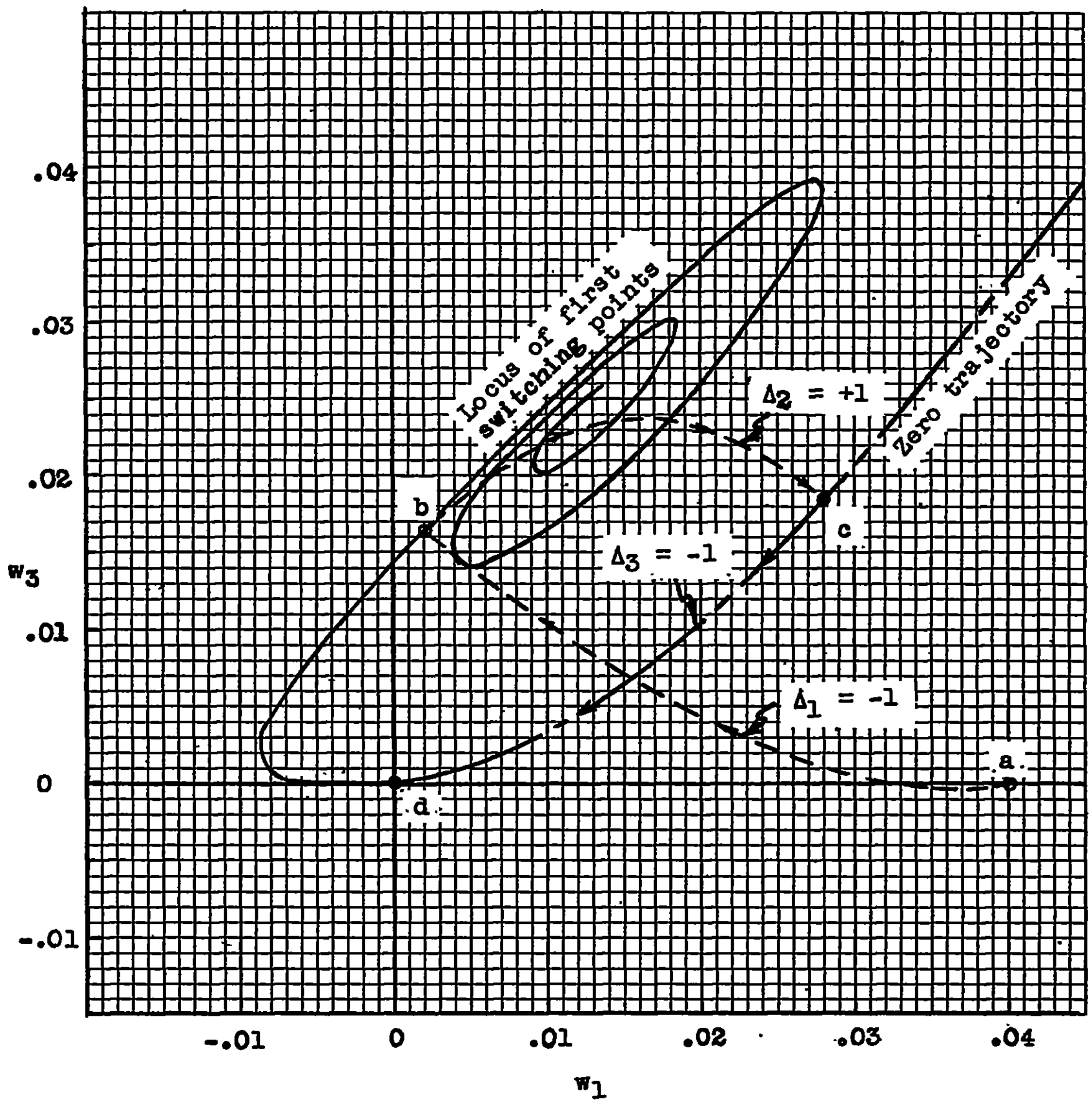

Figure 15.- A typical trajectory in the w_3w_1 plane for the optimum contactor normal-acceleration control system.

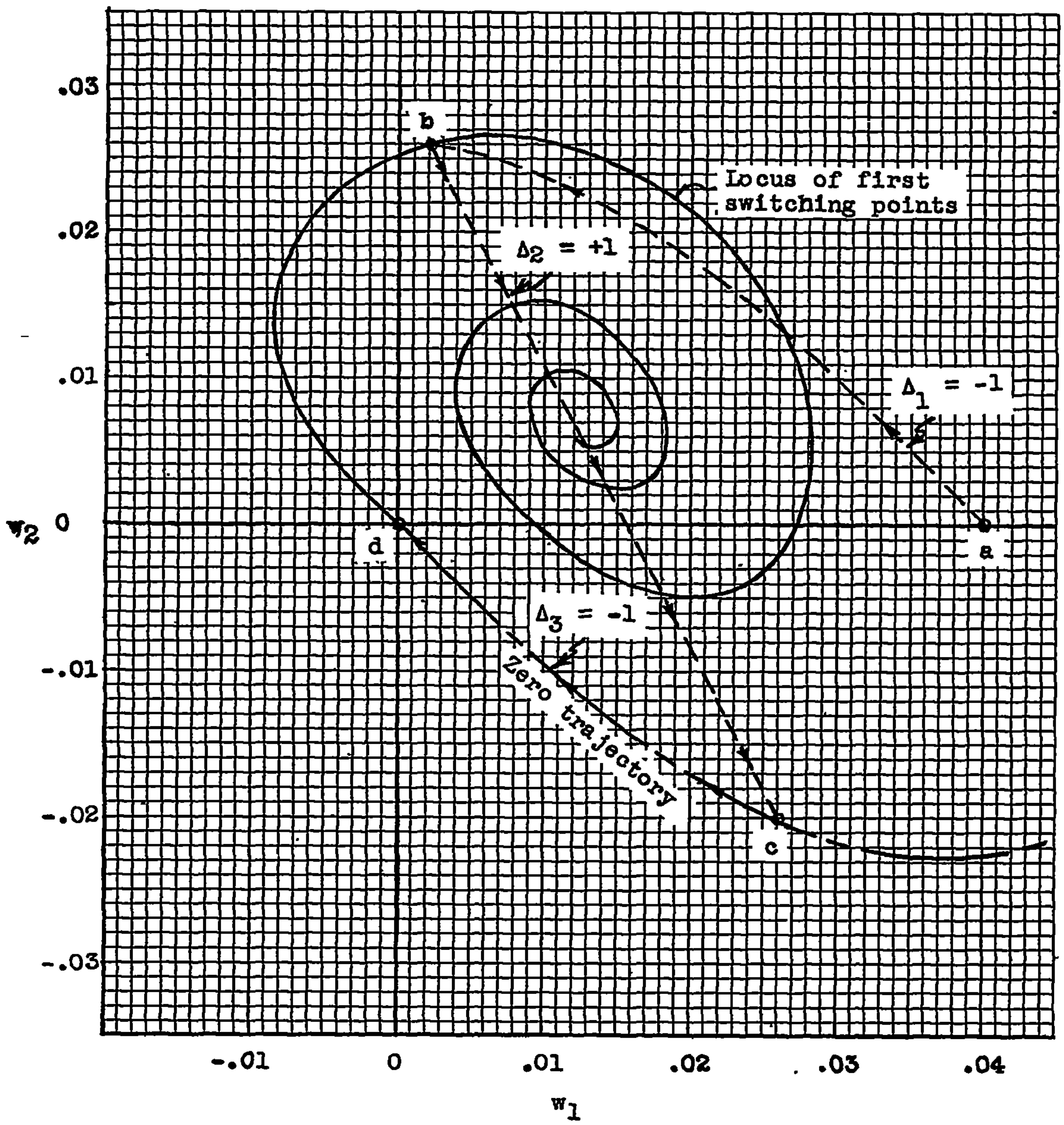

Figure 16.- A typical trajectory in the w_2w_1 plane for the optimum contactor normal-acceleration control system.

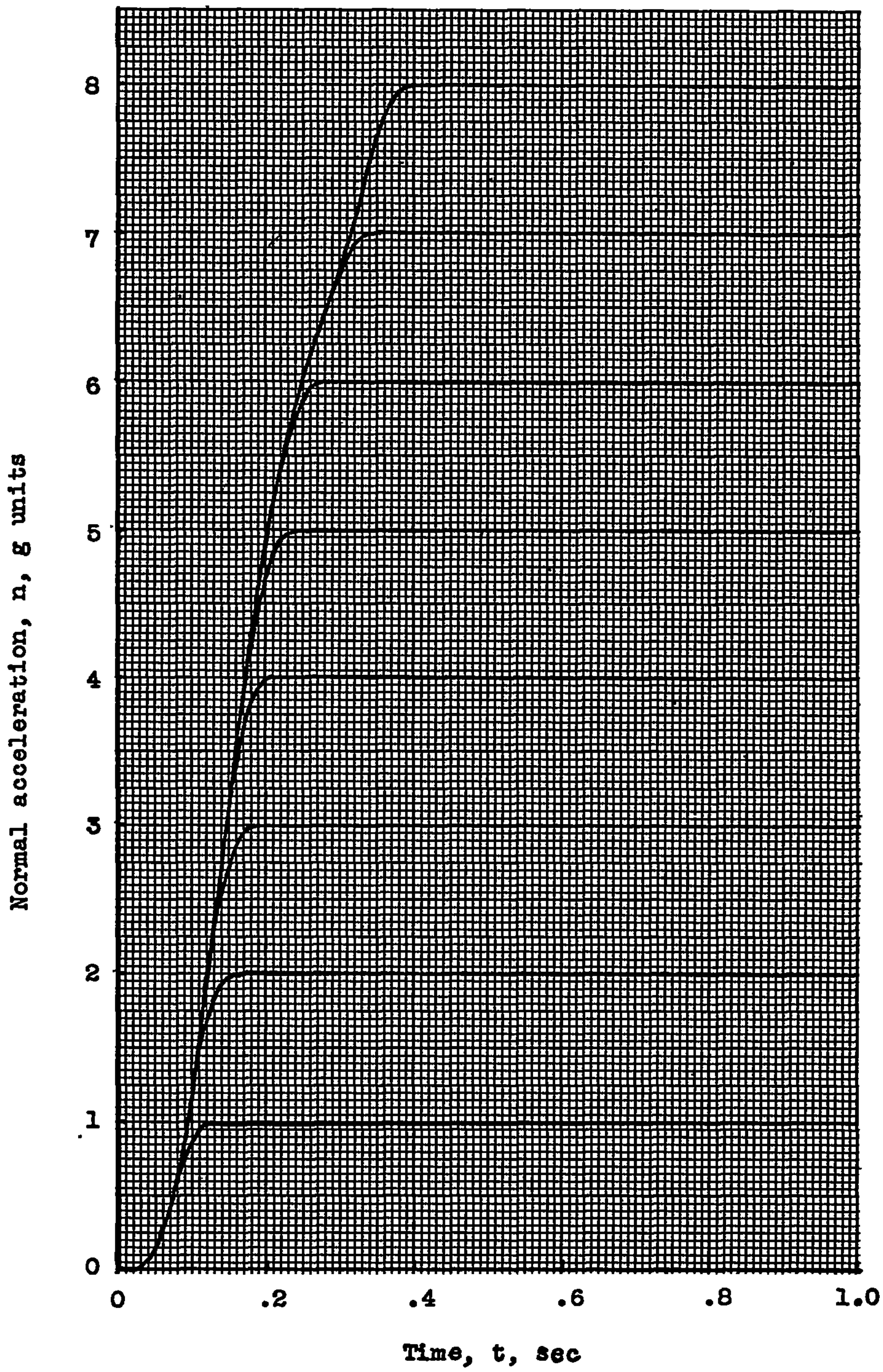

Figure 17.- Normal-acceleration transient responses of the optimum contactor normal-acceleration control system to step inputs of n_i.

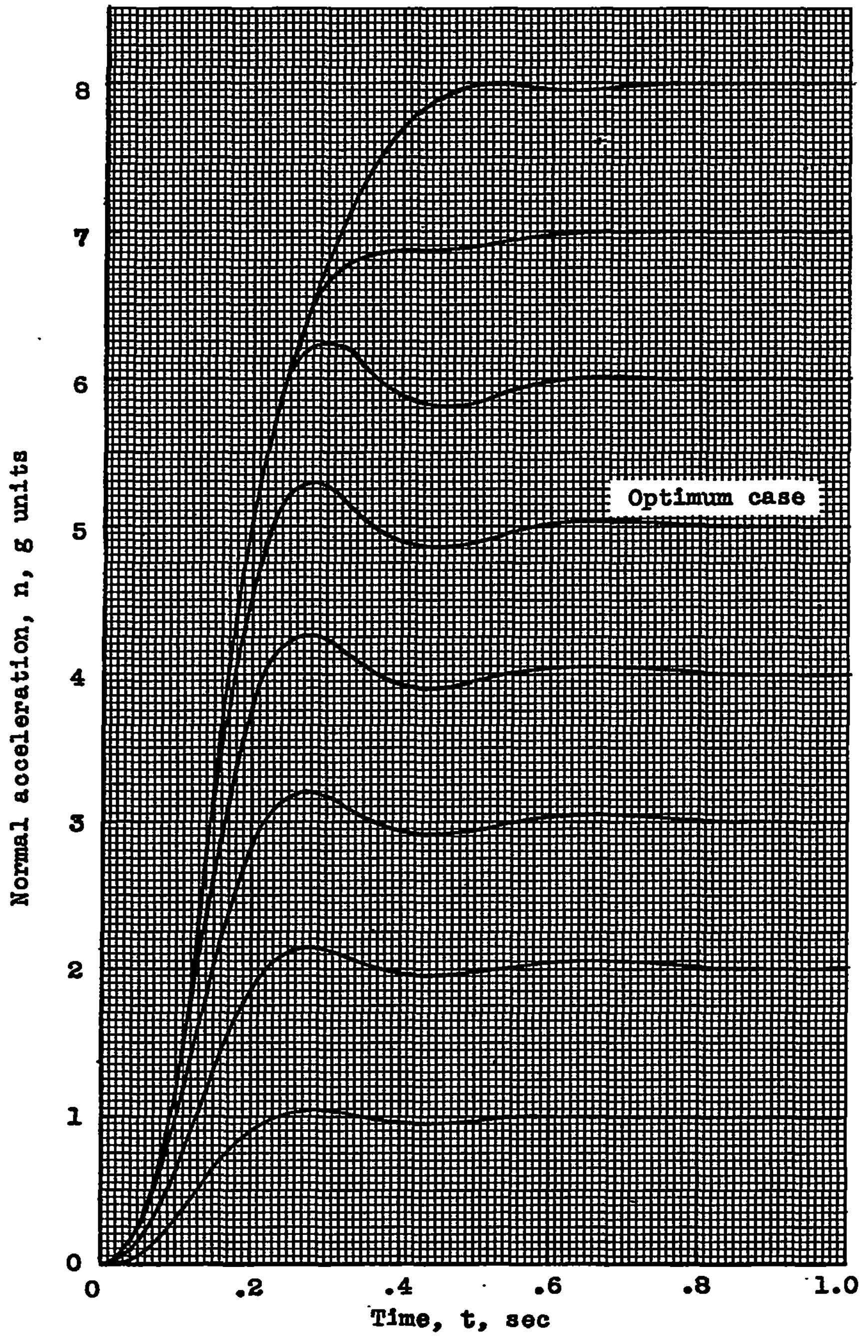

Figure 18.- Normal-acceleration transient responses of the limited-linear control system. The gains K_2 and K_3 were adjusted to yield a minimum value of $\int_0^t |\epsilon(t)| dt$ for an input signal n_1 of 5g.

NACA - Langley Field, Va.